Responses to Reviewers' Comments on Manuscript ACPD-2018-898

(Relative Humidity Effect on the Formation of Highly Oxidized Molecules and New Particles during Monoterpene Oxidation)

We are grateful for the reviewers' comments and we feel that our responses to these will greatly improve this manuscript. We have addressed the comments in the following paragraphs and made corresponding changes in the revised manuscript. Reviewer comments are shown as *blue italic text* followed by our responses. Changes are shown as underlined text in our responses and highlighted in the revised manuscript, the latter of which (along with supplemental information) is attached to the end of this document.

Reviewer #1:

The authors describe experimental findings from the ozonolysis of a-pinene, limonene and 3-carene from a flow through experiment conducted in the RH range of 3-90%. Runs have been carried out with the intention to study the RH-dependence of HOM formation of the terpenes and the resulting nucleation and particle growth. While HOM formation was found to be independent of RH, particle formation was clearly pushed back for rising RH. Some speculative explanations for that are presented. From my perspective, very interesting is the new transverse ionization inlet with the curtain gas unit, which could be an alternative to the commonly used Boulder-type inlet, as well as the experimental fact that HOM formation is totally free of water effects. I think that the manuscript meets the criteria for ACP and should be published in this journal. Some minor points should be considered before final acceptance is recommended:

1) Line 78-80: The authors mean that the intra-molecular H-shift, or RO2 isomerization, is characterized by a noticeable barrier making this unimolecular step clearly faster with rising temperature. I think it´s not good to say "autoxidation" has a barrier. Autoxidation stands more for the whole process.

Response: Thanks for the suggestion. We revised the original text accordingly: "The autoxidation of RO_2 includes intramolecular hydrogen shifts and O_2 additions. Several repetitions of the autoxidation cycle lead to a rapid increase in oxygen content as well as a decrease in saturation vapor pressure. Autoxidation was widely observed in condensed phase reactions, however, it was not considered in the gas phase previously due to the perception of a high barrier for the intramolecular hydrogen shift. This was confirmed by the fact that at higher temperatures, more HOMs are formed than at low temperatures (Frege et al., 2018).

Modeling studies now show that intramolecular hydrogen shifts are fast enough to compete with bimolecular sink reactions (Kurtén , et al., 2015)."

2) Line 85-86: The Boulder-type nitrate-CIMS by Eisele and Tanner does not suffer from a general problem with water vapour. Only in the case of relatively high RH in the reaction gas water cluster formation during gas expansion can disturb the analysis. Otherwise it works fine. That should be clearly stated at this point. Or have the authors other observations?

Response: We revised the original text accordingly: "HOM detection by the current commercially available CIMS inlet based on the design of Eisele and Tanner is subject to water cluster influence at high RH (Kürten et al., 2016)."

3) Line 90: In abstract a RH rangeof 3-90% is stated, and here 0-90%.

Response: Thanks for pointing this out. We confirm that the RH range in the manuscript is now consistently presented as 3-92%.

4) Line 114: It would be fine to have a table that compares parameters of the TI inlet with those of the commonly used boulder-type inlet, e.g. reaction times of the IMR, flows, HNO3 concentrations, TIC, detection limits, an estimate of wall losses for RO2s and closed-shell products, etc. Spectra of the same reaction gas recorded with both inlets would provide an impression how good the TI inlet works. Maybe the authors should think about a separate paper describing the TI inlet in detail. Could be important for the community.

Response: Thanks for the suggestion. We revised the text accordingly: "The calibration factors, defined as $C = [H_2SO_4]/([HSO_4^-]/[NO_3^-])$ (Eisele and Tanner, 1993), for the TI in this position and the commercial inlet were 3.25×10^{10} molecules cm^{-3} and 1.41×10^{10} molecules cm^{-3}, respectively. The lower calibration factor for the TI inlet is attributed to the shorter reaction time (~80 ms) compared to the commercial inlet (~200 ms). We note that the reaction time of the TI inlet can be further increased by positioning the ion source assembly further upstream relative to the inlet orifice, which would require a slight modification of the current design. The total ion counts (TIC) of the TI inlet are more than 5 times higher than the commercial inlet, which we attribute to the more direct path of ions through the ion source as well as the use of a Po^{210} radioactive source as compared to the soft X-ray in the commercial nitrate inlet. The limit of detection (LOD) for sulfuric acid, which is defined as three times the standard deviation of the background (Jokinen et al., 2012), is 9.3×10^{4}

molecules cm^{-3} and 1.26×10^5 molecules cm^{-3} for the TI and commercial inlets, respectively." With this revision, we have provided the information necessary to interpret our observations and thus we feel that a table is not necessary. However we will consider the reviewer's suggestion to perform additional characterizations of the TI inlet as well as comparisons to the "Boulder-type" inlet as part of a more detailed, future study.

5) Line 223: Can the authors derive HOM yields as a result of their experiments?

Response: An accurate estimate of the HOM yields requires several parameters, many of which must be experimentally determined and are not essential for addressing the main objectives of this study. The transmission efficiency in the TOF vacuum chamber must be determined. While some studies use the transmission curve published in previous literature (Heinritzi et al., 2016), we note that this can change significantly according to voltage settings applied to the TOF mass spectrometer. Another key parameter is the ionization efficiency for each compound, which can vary greatly for the HOM observed in this study: for example, NO_3^- based chemical ionization is reported to have relatively lower sensitivity to the OH-related RO_2 radicals compared to O_3-related RO_2 radicals (Berndt et al., 2016). Since we do not want to compromise our results by providing estimates that are based on many uncertain parameters, we have decided not to include yields in this manuscript and instead focus primarily on mechanism elucidation.

6) Line 228-229: Reaction of OH-derived RO2 radicals, C10H17Ox, with HO2 leads to H18 products, ROOH.

Response: The sentence was revised as: "As observed in previous studies, $C_{10}H_{15}O_{6,8,10,12}$ and $C_{10}H_{17}O_{5,7,9,11}$ comprised the O_3- and OH-related RO_2, respectively (Jokinen et al., 2014). $C_{10}H_{14}O_{5,7,9,11}$ comprised the O_3-related closed shell monomers, while $C_{10}H_{16}O_{6,8,10,12}$ and $C_{10}H_{18}O_{6,7}$ comprised the OH-related closed shell monomers (Ehn et al., 2014;Berndt et al., 2016)."

7) Line 258: Figure S5 should be given in the main body along with Fig.8. From my perspective, total SOA mass is almost water-independent within the experimental errors in the whole RH arrange while particle number drops down by a factor of two.

Response: We agree that the total SOA mass is almost water-independent. We revised the

text related to SOA mass generation accordingly: "SOA mass concentrations remains relatively constant". However, as also stated in the manuscript: "The variability in particle mass concentration as a function of RH for different experiments can be attributed to combined effects of gas phase reactions, condensed phase reactions, physical uptake of water, as well as the re-evaporation of semi-volatile compounds from the wall. We cannot accurately quantify these effects. As a result, although the measured SOA mass concentration remained relatively constant, we cannot draw accurate conclusions from this."

In consideration of article length, we feel that Figure 8 adequately expresses the RH influence on aerosol generation. Figure S5 is more about the details of the experiments, so we think it would be more appropriate to put it in the supplementary information. To clarify the data plotted in Figure 8, we have modified a sentence in the main body to show the size ranges of the generated SOA: "Figure 8 shows the integrated SOA particle number and mass concentrations over the observed diameter range of 10 - 100 nm." Later in that paragraph we state "Peaks in the particle number-size distributions were between 40 and 70 nm (Figure S5)."

8) Line 319: Here, reagent ion dependent sensitivity for different product classes should be mentioned that could lead to different results for different reagent ions.

Response: Thanks for the suggestion. The sentence was revised as: "This could be explained by a lower OH/O_3 ratio in our experiments, since unlike Berndt et al. we did not provide an extra source of OH to the flow tube. Also, Berndt and coauthors reported lower sensitivity of nitrate reagent ions to OH-related RO_2 compared to other reagent ions such as acetate."

Reviewer #2:

The study examines the influences of relative humidity (RH) on the formation of HOM and aerosol from the ozonolysis of three different monoterpenes. HOM have been shown to be central for particle formation over the last years, and therefore knowing their yields under different atmospherically relevant conditions is important. The influence of RH has clearly not been addressed in earlier studies, making this work timely and appropriate.

The paper is well-written and the presentation of results is clear and straight-forward. The strength of the paper lies in the finding that HOM yields do not change as a function of RH, and this analysis by itself makes the manuscript worthy of publishing in ACP. The results and subsequent discussion on number and mass formation seem much more speculative. Overall,

I have several comments that the authors need to address before potential publication.

Major Comments:

1. *RH control. In section 2.1, the authors describe that the RH in flow tube was achieved by mixing a humidified and a dry flow. The humidified flow was 6.5 LPM while the total in the flow tube was 8.5 LPM. Assuming these flows were at the same temperature (which one would hope) when entering the flow tube, then even if the humidified flow was fully saturated at RH=100%, then the maximum achievable RH should be 6.5/8.5 = 76%. However, the authors state that the RH was probed up to 92%. I do not see how this is possible, unless the humidified flow indeed was several degrees warmer when entering the flow tube. If this were the case, it would not be surprising that particle number formation decreased, as nucleation is an extremely temperature sensitive process.*

Response: As stated in the text, we used a temperature-controlled bubbler to provide the humid air. The first three stages of RH were generated with the bubbler at room temperature, and the fourth stage (85-92%) was generated by heating the bubbler to ~35 °C. The reviewer is correct that the only way to achieve this RH by mixing flows is for the humid air to enter the chamber as a slightly higher temperature than the dry monoterpene flow. Assuming saturation of the humid flow, we estimate that the temperatures of the humid and dry flows were 26 °C and 20 °C, respectively, for the high RH stage only (note: due to the 1 LPM sample flow of the ozone analyzers, the humid and dry flows were actually 6 and 2.5 LPM, respectively). Due to turbulent mixing conditions produced at the inlet end of the flow tube, we expect that the gas temperature quickly reaches the room temperature for the experiments conducted at the highest RH. It is important to note that the first three RH stages were generated at room temperature and the bubbler was heated up only for the highest RH stage, yet particle number concentrations decreased monotonically with each level of RH increase. Nevertheless we cannot discount the influence of temperature in the last RH stage experiments, so we have added the following text: "In order to achieve the highest relative humidity stage, the temperature of the humid flow was saturated at 26 °C before being mixed with room temperature air from the monoterpene source. This resulted in a slightly higher temperature at the inlet of the flow tube, which could contribute to lower nucleation rates (Burkholder et al., 2007). Nevertheless, over the range of the first three humidity stages, up to 65% RH, the gas temperature was constant before, during, and after reaction."

2. *In Figure 6b, when RH is 0, the mass concentration is steadily increasing over the course*

of nearly one hour. This is very surprising considering that the residence time in the flow tube is 1 minute. Clearly there is some memory effects, and this is not currently discussed at all in the manuscript. Accumulation of semi-volatile on walls is a common phenomenon, and can perhaps explain this behavior. Whatever the reason, it puts very high uncertainties on the results, considering that RH may influence the rate of (re-)evaporation from the walls. Are the measured SOA mass changes really significant when considering this?

Response: We agree that there may be some memory effects and the semi-volatile species may accumulate and re-evaporate from the wall. The re-evaporation rate could be affected by RH, and if true then this would have some influence on the measured SOA mass concentration. As we mentioned in the paper, this effect is not quantitatively evaluated in our current work. In fact, as we mentioned in the paper, the measured mass concentration likely depends on this effect plus gas phase reactions, gas-particle partitioning, condensed phase reactions, and physical uptake of water. With all these effects and uncertainties, we cannot draw conclusions as to the measured SOA mass concentrations. We have added some sentences in the paper to clarify this: "The variability in particle mass concentration as a function of RH for different experiments can be attributed to combined effects of gas phase reactions, condensed phase reactions, physical uptake of water, as well as the re-evaporation of semi-volatile compounds from the wall. We cannot accurately quantify these effects. As a result, although the measured SOA mass concentration remained relatively constant, we cannot draw conclusions from this observation. In contrast, while particle number concentrations may also be affected by the factors mentioned above, they decreased by a factor of 2~3 with increasing RH."

It is important to note, however, that this phenomenon does not impact our conclusions regarding HOM generation. As shown in section 3.6, almost all the main compounds are ELVOCs or LVOCs, which were not likely to re-evaporate from the wall.

3. *Particle number concentration was in excess of 1e6 cm^-3. At such high concentrations, couldn't nucleation "shut down" at a certain point just because the condensation sink starts to overwhelm the collisions between nucleating agents? Alternatively, the ultimately measured particle number might mainly be limited by coagulation between newly nucleated clusters/particles. While I am not an expert on nucleation, the extreme particle number concentration raise many questions about how far the absolute values can be compared directly, as done by the authors.*

Response: We agree that nucleation can "shut down" at a certain point because the

condensation sink starts to overwhelm the collisions between nucleating species. This is the reason we only detected the larger particles (10-100 nm) instead of the nucleation mode particles (<10 nm) at the end of the flow tube. It's very likely that new particle formation only happens at the entrance to the flow tube, while new particles formed at later stages will coagulate with the existing larger particles very quickly. Following this, particle number concentrations decrease due to coagulation and wall loss. The particle coagulation coefficient and wall loss coefficient are simple physical parameters and are well known to be unaffected by H_2O. The peak sizes in particle size distributions do not change much under different RH, especially in experiments without OH scavenger (Figure S5). As a result, we assume the particle coagulation term and wall loss term have linear effects on the particle number concentration for different RH. Based on these, the observed decreases in final particle number concentration with increasing RH should reflect the trend in new particle formation rate at different RH. Therefore we feel there is sufficient justification to compare number concentrations at different RH.

We have addressed this issue by confirming the following: (1) while absolute number concentrations are being referred to in the text, the conclusions drawn from the comparisons acknowledge the uncertainties associated with their changes, e.g., stating that concentrations change by factors of "2~3" rather than exact calculated values; (2) we remind the reader that changes in number concentration with RH can also be due to many of the factors that contribute to changes in mass concentration by including the following statement: "In contrast, while particle number concentrations may also be affected by the factors mentioned above, they decreased by a factor of 2~3 with increasing RH."

4. *Related to the precious point, the authors state that since the aerosol surface area is so much lower than the flow tube wall area, the dominant loss term for HOM will be wall loss. This statement seems completely illogical. How are the particles even formed in the flow tube if all ELVOC or LVOC would condense on the walls? The authors need to calculate the actual condensation sink (CS) produced by the particles and I think they will find that the lifetime of HOM due to CS is on the order of seconds, While wall loss will be a slower process. Calculating a coagulation sink in addition might also help address my earlier comment in nr 3.*

Response: We thank the reviewer for pointing out this oversight. Following the reviewer's guidance, we realized that the comparison between the wall surface area and particle surface

area cannot represent the relative importance of wall loss rate and condensation rate onto particles. We have calculated the condensation sink (CS) (Kulmala et al., 2001) and wall loss rate (W) (Crump and Seinfeld, 1981;Kürten et al., 2014) using the following equation:

$$\mathrm{CS} = 2\pi \mathrm{D} \sum_{d_p} \beta_{M,d_p} dp N_{d_p}$$

$$\mathrm{W} = \frac{2}{\pi} \cdot \frac{A_{chamber}}{V_{chamber}} \cdot \sqrt{k_e \cdot D}$$

Where, β_{M,d_p} is the transition correction factor; D is the diffusion coefficient of H_2SO_4, 8.5E-6 m^2 s^{-1}; $A_{chamber}$ and $V_{chamber}$ are the surface area and volume of the chamber; k_e is the eddy diffusion coefficient, which we use an empirical value of 0.001 s^{-1}.

The manuscript was revised as: "The condensation sink (CS) and wall loss rate for a compound with diffusion coefficient of 8.5×10^{-6} m^2 s^{-1} (e.g., sulfuric acid) were estimated using established methods (Kürten et al., 2014;Crump and Seinfeld, 1981;Kulmala et al., 2001). The calculated CS varied between 0.1-3.5 s^{-1} in different SOA generation experiments, much larger than the wall loss rate (< 0.01 s^{-1}). There was about 5-30% variation in CS in each SOA generation experiment from RH=3% to 92%. This amount of variation in CS does not seem to have a noticeable influence on the final concentration of HOMs. To further test the hypothesis that variations in condensation sink do not impact final HOM concentrations, particle free experiments were performed and, again, detected HOM concentrations did not change with RH (Figure 7)."

5. *Section 3.6 discusses volatility estimated of HOM. However, it seems the authors are not aware of the work by Kurtén et al. (2016), entitled "α-Pinene Autoxidation Products May not Have Extremely Low Saturation Vapor Pressures Despite High O:C Ratios". This work certainly needs to be discussed in conjunction with this section, as it raises considerable doubts about the applicability of SIMPOL to vapor pressure estimated of HOM. Using SIMPOL in this work is still completely appropriate, but the large uncertainties should be noted, Also other parts of section 3.6 are questionable, but primarily the authors need to revisit the discussion about oxidation state OSc. The formula they utilize (2*O:C-H:C) is not applicable in the case that molecules contain (hydro) peroxide functionalities. And according to Table S1, the authors assume this is the case for every molecule under discussion. This will require rewriting all parts where OSc is discussed.*

Response: Thanks for the suggestions. We were aware that the saturation vapor pressure

predicted from SIMPOL model may deviate from the real value. There are a lot of uncertainties not only from the method itself but also from simplification methods we used to estimate the functional groups. We revised the paper as "It has to be noted that the group contribution methods very likely underestimate the volatility of the α-pinene autoxidation products due to ignoring intramolecular H-bonding (Kurtén et al., 2016). There may be large uncertainties in SIMPOL method as well as in our functional group estimation process. As a comparison, the Molecular Corridor method (Li et al., 2016), which does not require information on functional groups, was used to estimate the saturation vapor pressure as well."

We agree that the existence of (hydro)peroxide functional groups will cause the $\overline{OS}_C$ to deviate from $\overline{OS}_C$ calculated with this formula *(2*O:C-H:C)*. The reason is that the oxygen atoms normally have an oxidation state of -2 in most of the functional groups, but have an oxidation state of -1 in (hydro)peroxide groups. Although the deviations from the formula *(2*O:C-H:C)* was small (within 0.1) in some cases, the (hydro)peroxide may have a bigger influence on $\overline{OS}_C$ if they are present in relatively higher abundance (Kroll et al., 2011), as in our case. We revised the manuscript as: "The average carbon oxidation state ($\overline{OS}c$) was calculated with Equation 3, in replacement of the commonly used formula ($\overline{OS}_C = 2\mathrm{O:C} - \mathrm{H:C}$), as the second oxygen atom in (hydro)peroxide group does not increase the carbon oxidation state. In equation 3, n_O, n_C, and n_H are the oxygen, carbon, and hydrogen numbers in the molecule; $n_{(hydro)peroxide}$ is the number of (hydro)peroxide groups in the molecule.

$$\overline{OS}_C = \frac{2n_O - n_{(hydro)peroxide} - n_H}{n_C} \quad \text{(Equation 3)}$$".

The values in Table S1 and Figure 9 were changed accordingly.

Minor Comments

6. *Section 2.1 describes the flow tube setup, but the description is in many places unclear and ambiguous. For the flows, 0.5 LPM is diluted by 6.5 LPM and then mixed with 2.5 LPM. This adds up to 9.5 LPM. But the total flow was apparently 8.5 LPM? There also seems to be different types of zero air used, although they are named the same. Is some of it bottled synthetic air? Finally, the author should clarify "Gas inlets to the flow tube were made from Teflon tubing that were capped and drilled with small wholes" better, since as written, it remains unclear to me exactly how this part of the setup looked.*

Response: We agree that the description of the flows was a little confusing. The O_3 analyzers

each require 1 LPM sample air, so this is why the total flow became 8.5 LPM. All of the zero air was generated by the zero air generator (model 737-30, Aadco Instruments). The diffusers consisted of capped ¼" Teflon tubes with ~1 mm holes drilled in the last ~2 cm of the tubes, and is based on the apparatus described and modeled in Ball et al. (1999).

In order to clarify the description we have rewritten the flow tube description as follows:

For these experiments, dry "zero air" was generated with a zero air generator (model 747-30, Aadco Instruments), with NOx and SO2 concentrations each specified to be less than 0.5 ppbv. The monoterpenes were injected into the flow tube using a syringe pump (model NE-300, New Era Pump Systems, Inc.) evaporated into a 2.5 LPM flow of dry zero air. O3 was generated by passing 0.5 LPM dry zero air (79% N2, 21% O2) over a Hg UV lamp (model 90-0004-04, UVP, LLC) and then diluted with 6.5 LPM of humidity-controlled zero air. A temperature-controlled bubbler filled with deionized water was used to generate humid air, and the prescribed RH was achieved by controlling the temperature of the bubbler. An ozone analyzer, described below, sampled at 1 LPM, resulting in a total flow rate of 8.5 LPM and a corresponding reaction time of ~60 s for each experiment. Gas inlets to the flow tube were made from 0.64 cm outside diameter Teflon tubes that were capped and drilled with ~1 mm holes to distribute sample air uniformly into the flow tube, as described and modeled in Ball, et al. (1999).

7. *There is variability in earlier literature about how to write the plural HOM. In some cases also the plural is "HOM", while in other studies they are "HOMs". However, the usage in many places in this work seems questionable. "HOMs dimers", "HOMs volatility", "HOMs production", etc, sound incorrect to me, and HOM should not be in plural form in these cases.*

Response: Thanks. All the "HOMs dimers", "HOMs monomers", "HOMs volatility", "HOMs production", "HOMs products", "HOMs formation", "HOMs generation", "HOMs partitioning", "HOMs concentration", "HOMs spectrum", "HOMs abundance", "HOMs signals" were changed to "HOM …".

8. *In the conclusion, lines 378-383 present various ways through which water could affect HOM formation, but then this is following by a sentence saying that none of them actually take place. Are those lines really needed, or are they just more likely to confuse a reader?*

Response: Line 378-383 is a summary of the possible water-influencing pathways. We feel it

is important to introduce these to the reader in order to understand the discussion that systematically analyzes each possible pathway (Line 383-393). Without this introduction, we feel that it would be harder for the reader to understand the context of our analysis.

9. *Line 139, the inlet flow to the mass spectrometer is given as 0,5 LPM, but is it not closer to 0.7 LPM? This is given in some earlier studies, and is closer to the theoretical value for a 0.3 mm orifice.*

Response: The inlet flow was not directly measured, but was subtracted from all the TI inlet flows by all the outlet flows and therefore is subject to measurement uncertainties (which is why we use the approximate symbol "~" in describing the flow). The important point of this section of the text is that the curtain flow exceeded the flow into the mass spectrometer, so we will accept the reviewer's suggestion and replace "~0.5" with the more generally-accepted "~0.7".

10. *Line 304. This is not a very clear sentence, but if I understand correctly, the hydroperoxide should be an alcohol?*

Response: Yes! "hydroperoxide" was revised as "hydroxyl".

11. *Figure 3. The legend says "upstram".*

Response: Thanks, corrected.

12. *Figure 4 need larger axis labels.*

Response: Thanks, revised.

13. *Figure 6c. The legend for the liens is incorrect. O3 radicals are given twice, as are OH monomers. They should be mixed.*

Response: Thanks, corrected.

14. *Figure 9. The molecule in blue in the top-most box: is the keto form more commonly depicted than the enol from given here ?*

Response: As suggested by the reviewer, we checked the literature and found that the aldehyde form is more commonly depicted than the enol form. We changed the related structure in Figure 9 and the volatility prediction accordingly.

15. *There are references to "Kurten at al (2012)" and "Kuerten et al (2016)". As these, to my understanding, are the same person, they should be spelled the same.*

Response: Thanks for the correction. All of "Kürten, Andreas" are uniformed as "Kürten";

All of "Kurtén, Theo" are uniformed as "Kurtén".

16. While the likelihood of misunderstandings about what particles are studied here is low, the word "aerosol" is not used before in section 2.3. I suggest to include it at least once at a much earlier stage.

Response: Thanks for the suggestion. The term "SOA" was introduced in the abstract as well as the introduction. The sentence in the abstract is "The ozonolysis of α-pinene, limonene, and $\triangle^3$-carene, with and without OH-scavenger, were carried out under low NOx conditions under a range of RH (from ~3% to ~92%) in a temperature-controlled flow tube to generate secondary organic aerosol (SOA)". We also corrected the first reference to SOA in the introduction (line 85) to "… secondary organic aerosol (SOA)".

Reviewer #3:

The Manuscript describes the RH effects on HOMs formed from oxidation reactions (ozone and OH) of monoterpenes and on the SOA formation. The authors used HRTOF-CIMS to measure gas phase HOMs (monomer and dimers). The main conclusion is that because HOMs are not affected by RH under the present experimental conditions, formation pathways of HOMs may not include water. The review believes this is a reasonable explanation, considering that the autoxidation reactions take place in the condensed phase and at high temperatures, where water is less available. Considering the increasingly important roles of HOMs in NPF and SOA formation, this conclusion is useful to the community.

Since the measured particles sizes in this study are between 20-100nm, it would be difficult to discuss the contribution of RH on NPF from these sizes. It is more likely that the precursors of nucleation (or NPF) and 20-100 nm particles have different volatilities and they may be even different precursors. Therefore, the RH effects on these aerosol particles are different from what the community considers regarding to RH effects on NPF (started in Introduction). Rather, the results shown here indicate the effects on SOA formation. So, I would suggest reorganize Introduction and results/discussion to focus on HOMs. Since RH varies in a large range in the atmosphere, it is still important to understand the effects of RH on HOMs formation.

Response: We agree with the reviewer that it is not correct to associate the formation rate of ~20 nm diameter particles with NPF rates, and we have been careful to avoid such comparisons. We do feel, however, that the observed trends in total particle number do reflect trends in NPF, once we have accounted for effects such as coagulation and wall losses. See our comments to Reviewer 2, Comment 3, above describing how we have addressed such effects. To summarize, we can assume that particle coagulation and wall loss are monotonically related to particle number concentration for different RH (that is, each

increases with increased number concentration and neither is greatly affected by RH). Based on this, the observed decreases in final particle number concentration with increasing RH should reflect the trend in new particle formation rate at different RH. Therefore we feel there is sufficient justification to associate changes in overall number concentrations with NPF.

(1) Line 38-42: The Amazon NPF or lack of it has little to do with RH, rather it is due to high condensation sink or the lack of nucleation precursors.

Response: As suggested by the reviewer, the Amazon example was removed.

(2) Line 60: Include Yu, H., (2012). "Effect of amines on the formation of sub-3 nm particles and their subsequent growth." Geophys. Res. Lett. 39: Doi: 10.1029/2011gl050099.

Response: Thanks, the recommended reference was added.

(3) Section 2.4. Indicate the exact equation that is used to calculate saturation mass concentrations (C). Later, it is stated that the functional groups are also considered, so it would be useful to show the calculation procedure.*

Response: The functional groups used for calculation was summarized in Table S1. As suggested by the reviewer, the calculation equation was added in the caption of Table S1: "The equation used for volatility calculation is $log_{10}P^0_{L,i}(T) = \sum_k v_{k,i} b_k(T)$, where $P^0_{L,i}(T)$ is the liquid vapor pressure of the compound. $v_{k,i}$ is the number of groups of type k, and $b_k(T)$ is the contribution by each group of type k. (Pankow and Asher, 2008)".

(4) Line 210: What is the source of e5 /cc of sulfuric acid?

Response: The trace amount of H_2SO_4 is generated by OH oxidation of SO_2. There is always a trace amount of SO_2 in the zero air, and the ozonolysis process will generate some OH radical in the experiments without OH scavenger which will lead to formation of H_2SO_4. To clarify this, we have edited the sentence in question as follows: [H2SO4], which arises from the oxidation of trace amounts of SO2 in the aero air, was ~105 molecules cm-3 and was always less than 3% of the most abundant C10 products, suggesting that sulfuric acid plays a negligible role in nucleation and cluster growth in our experiments.

(5) Line 231: Dimers are more abundant from OH oxidation. This is an interesting result, considering that HOMs formed from ozonolysis are found mostly during the nighttime, where NPF does not take place. So this may explain the importance of dimers on aerosol nucleation.

Response: In our manuscript, we indicate that $C_{20}H_{32}O_{6\text{-}13}$ generation is more abundant in

experiments without OH-scavenger, as compared to experiments with OH scavenger. This is because some of the $C_{20}H_{32}O_x$ is generated by the bimolecular reaction between an OH-derived RO_2 ($C_{10}H_{15}O_{2n}$) and an O_3-derived RO_2 ($C_{10}H_{17}O_{2m+1}$). We cannot conclude that dimer formation from OH chemistry is more than from O_3 chemistry, because there are other dimers formed, e.g.,$C_{20}H_{30}O_x$. Also, because we didn't perform the OH-only chemistry, we cannot compare the yield of OH and O_3 chemistry directly.

However, we did find that: "For the HOM products with identical $\overline{OSc}$, OH-derived HOMs have lower volatilities than O_3-derived HOMs due to a greater number of (hydro) peroxide groups. As a result, OH chemistry is suspected to be more likely to lead to NPF than O_3 chemistry, given the same level of oxidants and VOCs precursors."

(6) Lines 251-252: Show condensation sink, instead of surface area. The size distribution shows aerosol sizes are 20-100 nm, so condensation actually takes place effectively.

Response: Thanks for the suggestion. Following the reviewer's guidance and that of Reviewer 2 (see our response to Question 4), we realized that the comparison between the wall surface area and particle surface area cannot represent the relative importance of wall loss rate and condensation (on particles) rate. The manuscript was revised as: "The condensation sink (CS) and wall loss rate for a compound with diffusion coefficient of 8.5×10^{-6} m^2 s^{-1} (e.g., sulfuric acid) were estimated using established methods (Kürten et al., 2014;Crump and Seinfeld, 1981;Kulmala et al., 2001). The calculated CS varied between 0.1-3.5 s^{-1} in different SOA generation experiments, much larger than the wall loss rate (< 0.01 s^{-1}). There was about 5-30% variation in CS in each SOA generation experiment from RH=3% to 92%. This amount of variation in CS does not seem to have a noticeable influence on the final concentration of HOMs. To further test the hypothesis that variations in condensation sink do not impact final HOM concentrations, particle free experiments were performed and, again, detected HOM concentrations did not change with RH (Figure 7)."

(7) Lines 260-261: Indicate yields.

Response: The sentence was revised as: "The generated SOA particle number and mass concentrations for limonene (2.2-6.0 × 10^6 cm^{-3} for number concentrations and 470-1025 μg m^{-3} for mass concentrations) were ~3-12 times greater than for Δ^3-carene (0.3 - 2.0 × 10^6

cm^{-3} for number concentrations and 56-86 μg m^{-3} for mass concentrations) and α-pinene (0.4 - 2.2 × 10^6 cm^{-3} for number concentrations and 61-130 μg m^{-3} for mass concentrations).”

(8)Line 306: Decomposition to C5 HOMs. Is this new?

Response: The detection of C5-C9 HOMs during pinene oxidation is not new. As reported by Ehn and his coauthors (Ehn et al., 2012), $C_5H_6O_7$ is abundant in α-pinene oxidation, as well as some C7 - C9 fragments. However, the formation pathways were unclear. In our manuscript, we just gave a possible formation pathway of C5 - C9 – there may be other fragmentation pathways that we have not considered and that should be the focus of future studies.

References cited

Ball, S. M., Hanson, D. R., Eisele, F. L., and McMurry, P. H.: Laboratory studies of particle nucleation: Initial results for H2SO4, H2O, and NH3 vapors, J Geophys Res-Atmos, 104, 23709-23718, 10.1029/1999jd900411, 1999.

Berndt, T., Richters, S., Jokinen, T., Hyttinen, N., Kurtén, T., Otkjær, R. V., Kjaergaard, H. G., Stratmann, F., Herrmann, H., and Sipilä, M.: Hydroxyl radical-induced formation of highly oxidized organic compounds, Nature communications, 7, 13677, 2016.

Burkholder, J. B., Baynard, T., Ravishankara, A. R., and Lovejoy, E. R.: Particle nucleation following the O-3 and OH initiated oxidation of alpha-pinene and beta-pinene between 278 and 320 K, J Geophys Res-Atmos, 112, 10.1029/2006jd007783, 2007.

Crump, J. G., and Seinfeld, J. H.: TURBULENT DEPOSITION AND GRAVITATIONAL SEDIMENTATION OF AN AEROSOL IN A VESSEL OF ARBITRARY SHAPE, J Aerosol Sci, 12, 405-415, 10.1016/0021-8502(81)90036-7, 1981.

Ehn, M., Kleist, E., Junninen, H., Petäjä, T., Lönn, G., Schobesberger, S., Maso, M. D., Trimborn, A., Kulmala, M., and Worsnop, D.: Gas phase formation of extremely oxidized pinene reaction products in chamber and ambient air, Atmos Chem Phys, 12, 5113-5127, 2012.

Ehn, M., Thornton, J. A., Kleist, E., Sipila, M., Junninen, H., Pullinen, I., Springer, M., Rubach, F., Tillmann, R., Lee, B., Lopez-Hilfiker, F., Andres, S., Acir, I.-H., Rissanen, M., Jokinen, T., Schobesberger, S., Kangasluoma, J., Kontkanen, J., Nieminen, T., Kurtén, T., Nielsen, L. B., Jorgensen, S., Kjaergaard, H. G., Canagaratna, M., Dal Maso, M., Berndt, T., Petaja, T., Wahner, A., Kerminen, V.-M., Kulmala, M., Worsnop, D. R., Wildt, J., and Mentel, T. F.: A large source of low-volatility secondary organic aerosol, Nature, 506, 476-+, 10.1038/nature13032, 2014.

Eisele, F. L., and Tanner, D. J.: Measurement of the gas-phas concentration of H2SO4 and methane sulfonic-acid and estimates of H2SO4 production and loss in the atmosphere, J Geophys Res-Atmos, 98, 9001-9010, 10.1029/93jd00031, 1993.

Heinritzi, M., Simon, M., Steiner, G., Wagner, A. C., Kuerten, A., Hansel, A., and Curtius, J.: Characterization of the mass-dependent transmission efficiency of a CIMS, Atmos Meas Tech, 9, 1449-1460, 10.5194/amt-9-1449-2016, 2016.

Jokinen, T., Sipila, M., Junninen, H., Ehn, M., Lonn, G., Hakala, J., Petaja, T., Mauldin, R. L., Kulmala, M., and Worsnop, D. R.: Atmospheric sulphuric acid and neutral cluster measurements using CI-APi-TOF, Atmos Chem Phys, 12, 4117-4125, 2012.

Jokinen, T., Sipilä, M., Richters, S., Kerminen, V. M., Paasonen, P., Stratmann, F., Worsnop, D., Kulmala, M., Ehn, M., and Herrmann, H.: Rapid autoxidation forms highly oxidized RO2 radicals in the atmosphere, Angewandte Chemie International Edition, 53, 14596-14600, 2014.

Kroll, J. H., Donahue, N. M., Jimenez, J. L., Kessler, S. H., Canagaratna, M. R., Wilson, K. R., Altieri, K. E., Mazzoleni, L. R., Wozniak, A. S., Bluhm, H., Mysak, E. R., Smith, J. D., Kolb, C. E., and Worsnop, D. R.: Carbon oxidation state as a metric for describing the chemistry of atmospheric organic aerosol, Nature Chemistry, 3, 133-139, 10.1038/nchem.948, 2011.

Kulmala, M., Dal Maso, M., Makela, J. M., Pirjola, L., Vakeva, M., Aalto, P., Miikkulainen, P., Hameri, K., and O'Dowd, C. D.: On the formation, growth and composition of nucleation mode particles, Tellus B, 53, 479-490, 10.1034/j.1600-0889.2001.d01-33.x, 2001.

Kürten, A., Jokinen, T., Simon, M., Sipila, M., Sarnela, N., Junninen, H., Adamov, A., Almeida, J., Amorim, A., Bianchi, F., Breitenlechner, M., Dommen, J., Donahue, N. M., Duplissy, J., Ehrhart, S., Flagan, R. C., Franchin, A., Hakala, J., Hansel, A., Heinritzi, M., Hutterli, M., Kangasluoma, J., Kirkby, J., Laaksonen, A., Lehtipalo, K., Leiminger, M., Makhmutov, V., Mathot, S., Onnela, A., Petaja, T., Praplan, A. P., Riccobono, F., Rissanen, M. P., Rondo, L., Schobesberger, S., Seinfeld, J. H., Steiner, G., Tome, A., Troestl, J., Winkler, P. M., Williamson, C., Wimmer, D., Ye, P., Baltensperger, U., Carslaw, K. S., Kulmala, M., Worsnop, D. R., and Curtius, J.: Neutral molecular cluster formation of sulfuric acid-dimethylamine observed in real time under atmospheric conditions, P Natl Acad Sci USA, 111, 15019-15024, 10.1073/pnas.1404853111, 2014.

Kürten, A., Bergen, A., Heinritzi, M., Leiminger, M., Lorenz, V., Piel, F., Simon, M., Sitals, R., Wagner, A. C., and Curtius, J.: Observation of new particle formation and measurement of sulfuric acid, ammonia, amines and highly oxidized organic molecules at a rural site in central Germany, Atmos Chem Phys, 16, 12793-12813, 10.5194/acp-16-12793-2016, 2016.

Kurtén, T., Tiusanen, K., Roldin, P., Rissanen, M., Luy, J.-N., Boy, M., Ehn, M., and Donahue, N.: α-Pinene Autoxidation Products May Not Have Extremely Low Saturation Vapor Pressures Despite High O:C Ratios, The Journal of Physical Chemistry A, 120, 2569-2582, 10.1021/acs.jpca.6b02196, 2016.

Li, Y., Poeschl, U., and Shiraiwa, M.: Molecular corridors and parameterizations of volatility in the chemical evolution of organic aerosols, Atmos Chem Phys, 16, 3327-3344, 10.5194/acp-16-3327-2016, 2016.

Pankow, J. F., and Asher, W. E.: SIMPOL. 1: a simple group contribution method for predicting vapor pressures and enthalpies of vaporization of multifunctional organic compounds, Atmos Chem Phys, 8, 2773-2796, 2008.

Relative Humidity Effect on the Formation of Highly Oxidized Molecules and New Particles during Monoterpene Oxidation

Xiaoxiao Li[1,2], Sabrina Chee[1], Jiming Hao[2], Jonathan P. D. Abbatt[3], Jingkun Jiang[2*], and James N. Smith[1*]

[1]Chemistry Department, University of California, Irvine, CA 92697, USA

[2]State Key Joint Laboratory of Environment Simulation and Pollution Control, School of Environment, Tsinghua University, Beijing, 100084, China

[3]Department of Chemistry, University of Toronto, Toronto, Canada

*: *Correspondence to*: J. N. Smith (jimsmith@uci.edu) and J. Jiang (jiangjk@tsinghua.edu.cn)

Abstract. It has been widely observed around the world that the frequency and intensity of new particle formation (NPF) events are reduced during periods of high relative humidity (RH). The current study focuses on how RH affects the formation of highly oxidized molecules (HOMs), which are key components of NPF and initial growth caused by oxidized organics. The ozonolysis of α-pinene, limonene, and Δ^3-carene, with and without OH-scavenger, were carried out under low NOx conditions under a range of RH (from ~3% to ~92%) in a temperature-controlled flow tube to generate secondary organic aerosol (SOA). A Scanning Mobility Particle Sizer (SMPS) was used to measure the size distribution of generated particles and a novel transverse-ionization chemical ionization inlet with a high-resolution time-of-fight mass spectrometer detected HOMs. A major finding from this work is that neither the detected HOMs nor their abundance changed significantly with RH, which indicates that the detected HOMs must be formed from water-independent pathways. In fact, the distinguished OH- and O_3-derived peroxy radicals (RO_2), HOM monomers, and HOM dimers could mostly be explained by the autoxidation of RO_2 followed by bimolecular reactions with other RO_2 or hydroperoxy radicals (HO_2), rather than from a water-influenced pathway like through the formation of a stabilized Criegee intermediate (sCI). However, as RH increased from ~3% to ~92%, the total SOA number concentrations decreased by a factor of 2-3 while SOA mass concentrations remains relatively constant. These observations show that, while high RH appears to inhibit NPF as evident by the decreasing number concentration, this reduction is not caused by a decrease in RO_2-derived HOM formation. Possible explanations to these phenomena were discussed.

1 Introduction

New particle formation (NPF) is ubiquitous around the world (Kulmala et al., 2004). Newly formed particles contribute greatly to global particle populations and can grow further to act as cloud condensation nuclei (CCN), thereby influencing clouds and climate (Makkonen et al., 2012; Merikanto et al., 2009; Dunne et al., 2016). NPF characteristics vary from site to

site because of varying precursors and atmospheric conditions. It has been widely observed that the intensity (Sihto et al., 2006; Dada et al., 2017) and frequency (Dada et al., 2017; Boy and Kulmala, 2002; Hyvönen et al., 2005) of continental NPF are reduced during periods of high RH, resulting in reduced ultrafine particle number concentrations during these periods (Weber et al., 1997). For example, 20 years of observations in the boreal forest at Hyytiälä, Finland, showed that NPF is more likely to happen during periods of low ambient RH (Dada et al., 2017). In urban areas, NPF also favors low RH (Cai et al., 2017; Shen et al., 2011). Despite the low continental NPF event frequency at high RH, NPF has still been observed in the free troposphere in vicinity of clouds, where RH is extremely high (Weber et al., 1999) and in coastal and marine areas where RH is typically greater than 90% (O'Dowd et al., 1998).

The widely observed anti-correlation between NPF and RH in the field experiments can be attributed to the indirect influence of water. For example, high RH often corresponds to greater cloud cover, which can lead to lower ground-level concentrations of photo-oxidized precursors such as H_2SO_4 and HOMs as well as an increased condensation sink that leads to scavenging of precursors and clusters (Hamed et al., 2011). On the other hand, water vapor may also directly influence NPF by regulating the formation of gas phase precursors or by participating in cluster formation. For example, chamber and model experiments on the binary sulfuric acid-water system have demonstrated positive relationships between particle formation rate and RH (Duplissy et al., 2016; Merikanto et al., 2016). While in the ternary (H_2SO_4/MSA-H_2O-Amine/NH_3) system, H_2O was reported to have either positive (Chen et al., 2015) or negative (Napari et al., 2002) effects on NPF. Some studies have hypothesized that high water content might suppress the formation of NPF-related organics from the oxidation of biogenic precursors (Hyvönen et al., 2005; Boy and Kulmala, 2002). However, no direct evidence of this has been provided.

Although sulfuric acid has been recognized as the most important precursor of new particle formation, it alone can't explain the rapid formation and growth rates observed in the field (Kuang et al., 2008). Organic compounds, ammonia, amines, and water are also likely involved (Zhang et al., 2012; Chen et al., 2012; Yu et al., 2012). Organics have been shown to be very important for cluster formation and stabilization in theoretical studies (Ortega et al., 2016; Donahue et al., 2013), laboratory experiments (Tröstl et al., 2016; Schobesberger et al., 2013) and field measurements (Bianchi et al., 2016; Hoffmann et al., 2001; Metzger et al., 2010). Organics can either form clusters with sulfuric acid or purely with themselves (Zhao et al., 2013; Zhao et al., 2009). They can also contribute significantly to the condensational growth of newly formed particles, determining particle growth rates, particle lifetime, and global particle and CCN concentrations (Donahue et al., 2011; Vehkamäki and Riipinen, 2012). The ability of organics to take part in particle formation and condensational growth depends

on their volatility as well as reactivity. HOMs, such as extremely low volatility organic compounds (ELVOCs, saturation mass concentration (C^*) < 3×10^{-4} μg m^{-3}) or low volatility organic compounds (LVOCs, 3×10^{-4} < C^* < 0.3 μg m^{-3}), are likely contributors to NPF (Donahue et al., 2012; Ehn et al., 2014).

Despite its large contribution to NPF, the direct measurement of HOMs has long been a challenge because of their low atmospheric concentrations, low volatilities, and short lifetimes. Recently, the development of the high resolution time-of-flight chemical ionization mass spectrometer (HRToF-CIMS) overcame this barrier and made the measurement and identification of HOMs feasible (Junninen et al., 2010; Jokinen et al., 2012). HOMs from both monoterpene and aromatic oxidation showed high O/C ratios of >0.7 - 0.8, and were present as monomers, dimers and even higher order clusters (Molteni et al., 2018; Ehn et al., 2012). These high O/C ratios could not be explained by any of the formerly known oxidization pathways unless the autoxidation of RO_2 was taken into consideration (Crounse et al., 2013; Barsanti et al., 2017). The autoxidation of RO_2 includes intramolecular hydrogen shifts and O_2 additions. Several repetitions of the autoxidation cycle lead to a rapid increase in oxygen content as well as a decrease in saturation vapor pressure. Autoxidation was widely observed in condensed phase reactions, however, it was not considered in the gas phase previously due tof the perception of a high barrier for the intramolecular hydrogen shift. This was confirmed by the fact that at higher temperatures, more HOMs are formed than at low temperatures (Frege et al., 2018). Modeling studies now show that intramolecular hydrogen shifts are fast enough to compete with bimolecular sink reactions (Kurten et al., 2015).

Since most laboratory experiments related to the formation of HOMs have been conducted under conditions of constant RH, usually low or medium RH of less than 60% (Ehn et al., 2012; Zhang et al., 2015), it was still unknown whether and how water vapor might impact HOM formation. High RH conditions are difficult to achieve in chamber experiments without significantly changing temperature and pressure. In addition, HOM detection by the current commercially available CIMS inlet based on the design of Eisele and Tanner is subject to water cluster influence at high RH (Kürten et al., 2016).

In this research, three different endocyclic monoterpenes, α-pinene, limonene and $\triangle^3$-carene were reacted with ozone, with and without hydroxyl radical (OH) scavengers, in a reaction flow tube to generate secondary organic aerosol (SOA). RH influences on HOM formation and organic-driven NPF were studied under a range of RH from ~3% to ~92%. Generated closed-shell HOMs and RO_2 were measured using a home-built CIMS inlet coupled to a HRToF mass spectrometer (LTOF mass analyzer, Tofwerk AG). The CIMS inlet effectively reduced water clustering onto ions sampled into vacuum, thus removing sample artifacts caused by high water vapor levels. Water vapor influence on the formation of RO_2, HOM

monomers and HOM dimers were studied. The volatility of O_3- and OH-derived closed-shell HOMs were estimated with a group contribution-based model (SIMPOL) and a recently developed statistical model to study the potential contribution of O_3 and OH initiated chemistry on NPF.

2 Methods

2.1 Flow tube reactor

The experiments were performed in a laminar flow tube reactor consisting of a 150 cm long Pyrex glass cylinder with a volume of 8.5 dm^3 (Figure 1). The flow tube was located in a temperature controlled room (T = 293 ± 2 ℃) and was covered so that all experiments were performed under dark conditions. For these experiments, dry "zero air" was generated with a zero air generator (model 747-30, Aadco Instruments), with NOx and SO_2 concentrations each specified to be less than 0.5 ppbv. The monoterpenes were injected into the flow tube using a syringe pump (model NE-300, New Era Pump Systems, Inc.) evaporated into a 2.5 LPM flow of dry zero air. O_3 was generated by passing 0.5 LPM dry zero air (79% N_2, 21% O_2) over a Hg UV lamp (model 90-0004-04, UVP, LLC) and then diluted with 6.5 LPM of humidity-controlled zero air. A temperature-controlled bubbler filled with deionized water was used to generate humid air, and the prescribed RH was achieved by controlling the temperature of the bubbler. An ozone analyzer, described below, sampled at 1 LPM, resulting in a total flow rate of 8.5 LPM and a corresponding reaction time of ~60 s for each experiment. Gas inlets to the flow tube were made from 0.64 cm outside diameter Teflon tubes that were capped and drilled with ~1 mm holes to distribute sample air uniformly into the flow tube, as described and modeled in Ball et al., (1999). The uniform distributions of O_3 and H_2O in the flow tube were confirmed by measuring [O_3] and RH at the different locations prior to the experiments. In every experiment, RH was adjusted to be constant for at least 30 min for each of the four RH steps (3-5%, 30-38%, 58-65%, 85-92%). In order to achieve the highest relative humidity stage, the temperature of the humid flow was saturated at 26 ℃ before being mixed with room temperature air from the monoterpene source. This resulted in a slightly higher temperature at the inlet of the flow tube, which could contribute to lower nucleation rates (Burkholder et al., 2007). Nevertheless, over the range of the first three humidity stages, up to 65% RH, the gas temperature was constant before, during, and after reaction. At the beginning of the experiments, the inner wall of the reactor was washed with ultra-pure water. All of the flow rates were calibrated before and during the experiments.

2.2 Instrumentation

2.2.1 Transverse Ionization – Chemical Ionization Mass Spectrometer

A self-designed and home-built chemical ionization inlet, called Transverse Ionization (TI) inlet (Figure 2 and Figure S1), was used in front of the LTOF mass analyzer. The TI design is similar to those of the Ambient-pressure Proton transfer Mass

Spectrometer (AmPMS) (Hanson et al., 2011) and the cluster-CIMS (Zhao et al., 2010). In the TI inlet, a 4 - 10 LPM flow of sample air is passed across the inlet orifice of the mass spectrometer, where it encounters an orthogonal, 1 LPM reagent ion gas flow consisting N_2 containing ionized nitrate ions (NO_3^-) as well as potential cluster ions $(HNO_3)_nNO_3$ with n = 1-3. For the current study, the sample flow to the inlet was set to 4.5 LPM. Chemical ionization occurs at atmospheric pressure and temperature. The reagent gas is generated by passing 3 ccm of N_2 over a small vial containing nitric acid, which is then ionized by a 370 MBq Po^{210} radioactive source (model P-2021, NRD, LLC). An additional flow of N_2 can be added to the reagent gas to change the reagent ion concentration, and the assembly can be adjusted to vary ion-molecule reaction time. The latter can be controlled by adjusting the sample and reagent gas flow rates or by applying different voltages to the ionization source and the main inlet block. To minimize the diffusion loss in sample lines, the inlet of the TI source was connected to the flow tube outlet by a short (~10 cm) piece of electro-polished stainless steel tubing. Compared to the widely used commercial nitrate inlet patterned after the design by Eisele and Tanner (1993) and marketed by Aerodyne, Inc., no additional sheath flow is required thus any impurities potentially introduced by the sheath flow are eliminated. Some flow disturbance may occur where the sample flow encounters the transverse reagent flow, which may lead to non-ideal behavior. However, even at the maximum total flow of 11 LPM, the reynolds number in this region is ~500 thus turbulence is not expected to be significant.

Another unique aspect of the TI design is the use of an N_2 curtain gas in front of the inlet orifice to the mass spectrometer to reduce water clustering on reagent and sample ions. Water clusters are expected to form at high RH mainly during the free-jet expansion of the sampled gas on the vacuum side of the orifice plate (Thomson and Iribarne, 1979). The presence of these clusters makes the identification and quantification of both sample and reagent ions challenging (Kulmala et al., 2014; Lee et al., 2014; Kürten et al., 2016; Ehn et al., 2014). Figure 2 shows the details of the TI source that address this issue. Small holes drilled in a radial channel blow N_2 uniformly in front of the orifice plate so that only sampled ions and this clean N_2 gas pass into the vacuum chamber. Since the sampling flow rate of the mass spectrometer is ~0.7 LPM when using 0.3 mm orifice, the N_2 curtain flow is set to be 1 LPM to overflow the region surrounding the orifice. By applying voltages to the ion source and the block, the ions can be efficiently guided into the mass spectrometer while neutral molecules such as water vapor are prevented from entering by the N_2 curtain gas.

This TI inlet is suitable to all types of reagent ion chemistry, e.g. NO_3^-, I^-, and H_3O^+. Nitrate ion chemistry was used as the reagent ion in these experiments, which is selective to highly oxidized molecules that have at least two hydroperoxy (-OOH) groups or some other H-bond-donating groups (Hyttinen et al., 2015). HOM monomers, HOM dimers and highly oxidized

150 RO_2 radicals can also be measured using nitrate ion chemistry.

151

152 **2.2.2 Other measurements**

153 Ozone concentrations were measured with two ozone analyzers (model 106L, 2B Technology) at the inlet and outlet of the
154 flow tube. The sampling flow of each analyzer is 1 LPM. The two ozone analyzers were intercompared prior to the
155 experiments and the difference was within 5 ppbv when $[O_3] < 1000$ ppbv. A Scanning Mobility Particle Sizer (SMPS),
156 consisting of a Po210 bipolar neutralizer, a nano-Differential Mobility Analyzer (nano-DMA; model 3081, TSI, Inc.), and a
157 condensation particle counter (MCPC; model 1720, Brechtel Manufacturing) were used to measure the number-size
158 distribution of particles, which is later used to deduce the total particle number and mass concentrations (the latter assumes a
159 uniform density for organic particles of 1.2 g cm^{-3}). The sampling flow rate of the MCPC was 0.3 LPM and the sheath and
160 excess flows of the nano DMA were set to 3 LPM. The flow tube particle number-size distribution was measured without
161 further drying to get a more accurate measure of the actual particle surface area and volume, which are important for HOM
162 partitioning, and also to prevent particle evaporation during the measurements.

163

164 **2.3 Experimental conditions**

165 Three monoterpenes were used in our experiments (see Table 1), α-pinene, limonene and Δ^3-carene. Oxidation by ozone is
166 believed to dominate over other oxidation radicals (i.e., OH or NO_3) in forming SOA under atmospheric conditions
167 (Atkinson and Arey, 2003). Ozonolysis of alkenes generates a substantial amount of OH, leading to products that are
168 produced by a combination of O_3 and OH oxidation. For some experiments, in order to isolate oxidation by O_3, cyclohexane
169 (see Table 1 for mixing ratios) was premixed with the monoterpene and added to the flow tube as an OH scavenger. For other
170 experiments, the combination of OH and O_3 chemistry were investigated to study atmospheric oxidation chemistry more
171 representative of ambient air. The "high concentration" experiments were conducted with similar mixing ratios of
172 monoterpene (~1100ppb) and O_3 (~900ppb). The "low concentration" experiments were conducted to study the particle-free
173 chemical processes with initial concentrations of monoterpenes and O_3 shown in Table 1. Since wall losses should be
174 comparable for different precursors as a function of RH, it was not taken into consideration in our analysis of HOM
175 production.

176

177 **2.4 HOM volatility predictions**

178 The SIMPOL.1 method (Pankow and Asher, 2008) and the molecular corridor method (Li et al., 2016) were used to predict
179 the saturation mass concentrations (C*) of some of the detected OH- and O_3-related HOMs. SIMPOL.1 is a group

contribution method and requires information on molecular structure, while the molecular corridor method only requires the molecular formulae. Both methods are semi-empirical and based on volatility data from hundreds or thousands of compounds. The calculated volatilities were then applied to the two-dimensional volatility basis set (2D-VBS) (Donahue et al., 2012) to explore the likelihood that the products participate in the initial stages of nanoparticle growth.

3 Results and discussion

3.1 TI-CIMS performance

When comparing the TI inlet with the commercial nitrate inlet in measuring α-pinene ozonolysis products, both inlets produced identical mass spectra. The sensitivities of both inlets to H_2SO_4 were determined using a home-built H_2SO_4 calibration system (Figure S2) based on the design of Kürten et al. (2012). Figure 3 summarizes the results of these calibrations. The position of the ion source assembly relative to the inlet orifice is critical for determining the sensitivity of the TI inlet. When the ion source is placed 0.5 cm upstream along the sample flow axis and 5 cm away from the inlet orifice along the reagent ion flow axis (configuration shown in Figure 2), the instrument is at its most sensitive. The calibration factors, defined as $C = [H_2SO_4]/([HSO_4^-]/[NO_3^-])$ (Eisele and Tanner, 1993), for the TI in this position and the commercial inlet were 3.25×10^{10} molecules cm^{-3} and 1.41×10^{10} molecules cm^{-3}, respectively. The lower calibration factor for the TI inlet is attributed to the shorter reaction time (~80 ms) compared to the commercial inlet (~200 ms). We note that the reaction time of the TI inlet can be further increased by positioning the ion source assembly further upstream relative to the inlet orifice, which would require a slight modification of the current design. The total ion counts (TIC) of the TI inlet are more than 5 times higher than the commercial inlet, which we attribute to the more direct path of ions through the ion source as well as the use of a Po^{210} radioactive source as compared to the soft X-ray in the commercial nitrate inlet. The limit of detection (LOD) for sulfuric acid, which is defined as three times the standard deviation of the background (Jokinen et al., 2012), is 9.3×10^4 molecules cm^{-3} and 1.26×10^5 molecules cm^{-3} for the TI and commercial inlets, respectively.

After applying the N_2 curtain gas flow, the TIC recorded by the TI-CIMS decreased significantly. This was compensated for by increasing the ion source and reaction chamber voltages that direct ions to the orifice (Figure S3). When RH ≈ 90%, the reagent ion mass spectrum was dominated by water clusters $(H_2O)_m(HNO_3)_nNO_3^-$ (m = 0-30, n = 0-2) if no N_2 curtain flow was applied (Figure 4a). The reagent ions NO_3^-, $HNO_3NO_3^-$ and $(HNO_3)_2NO_3^-$ decreased as RH increased, with $[(HNO_3)_2NO_3^-]$ and $[HNO_3NO_3^-]$ decreasing much faster than $[NO_3^-]$. In contrast, after 1 LPM N_2 curtain flow was applied to the inlet, most of the water clusters were removed (Figure 4b). The reagent ions, sample ions and TIC remained stable as RH

increased, which resulted in a reliable measurement of HOM concentrations as a function of RH. The result that the N_2 curtain flow eliminated water clustering to a large extent confirms that most of the water clusters in the spectrum were produced during the free-jet expansion into vacuum instead of formed in the ion-molecular reagent region.

3.2 Identification of HOM spectrum

Figure 5 shows the average mass spectra of the HOM dimers and Figure S4 shows the average mass spectra of the HOM monomers and RO_2 radicals for each of the six particle generation experiments. More than 400 peaks were identified in each spectrum, the majority of which were clusters with NO_3^- or $HNO_3NO_3^-$. $[H_2SO_4]$, which arises from the oxidation of trace amounts of SO_2 in the aero air, was ~10^5 molecules cm^{-3} and was always less than 3% of the most abundant C_{10} products, suggesting that sulfuric acid plays a negligible role in nucleation and cluster growth in our experiments. After subtracting the reagent ions (NO_3^- or $HNO_3NO_3^-$), molecular formulae for organics with an odd number of H atoms were assigned to radicals, which are generally difficult to detect experimentally (Rissanen et al., 2015), and formulae with an even number of H atoms were assigned to closed-shell molecules. Most of the HOM products from the three endocyclic monoterpenes were very similar, while the relative abundance of different HOMs was quite different, indicating similar reaction pathways but different branching ratios in the reaction mechanisms. The main products were $C_{5\text{-}10}H_{6\text{-}16}O_{3\text{-}10}$ for closed shell monomers and RO_2 and $C_{15\text{-}20}H_{22\text{-}34}O_{6\text{-}18}$ for closed shell dimers. Among these, C_{10} and C_{20} compounds were the most abundant. $C_{5\text{-}9}$ products could be formed from O_3 attack on the less reactive exocyclic carbon double bond or the decomposition of intermediate radicals. Some fragments were found to be unique for specific monoterpene precursors. For instance, $C_5H_6O_7$ (m/z 240) was much more abundant in α-pinene oxidation than from other two precursors, which might be a tri-carboxylic acid (Ehn et al., 2012).

Comparing total HOM abundance for the three monoterpene oxidation reactions, limonene created the most, followed by α-pinene and then Δ^3-carene. This is in qualitative agreement with prior studies (Jokinen et al., 2014; Ehn et al., 2014). The total dimer signal intensity was 15-30% of monomers for all three monoterpenes. Experiments with an OH scavenger generated fewer HOMs than those without OH scavengers.

As observed in previous studies, $C_{10}H_{15}O_{6,8,10,12}$ and $C_{10}H_{17}O_{5,7,9,11}$ comprised the O_3- and OH-related RO_2, respectively (Jokinen et al., 2014). $C_{10}H_{14}O_{5,7,9,11}$ comprised the O_3-related closed shell monomers, while $C_{10}H_{16}O_{6,8,10,12}$ and $C_{10}H_{18}O_{6,7}$ comprised the OH-related closed shell monomers (Ehn et al., 2014; Berndt et al., 2016). When comparing the average spectra with and without OH scavenger, no obvious differences were seen for OH-related RO_2 or monomers (Figure S4). In

contrast, for dimers we found that $C_{20}H_{32}O_{6\text{-}13}$ were more abundant in experiments without OH scavenger (Figure 5). The formation of these dimers can be explained by the reaction of one OH-related RO_2 with one O_3-derived RO_2 (see Section 3.5), and can therefore be considered as markers for combined OH and O_3 chemistry. As HOM dimers are generally less volatile than monomers with identical O/C ratio, rapid production of dimers is believed to play a more important role in initial particle formation and growth (Zhang et al., 2015).

3.3 RH influence on HOM generation

Figure 6 shows a time series of experimental parameters, particle size distribution, and key ions from the limonene ozonolysis experiment with OH scavenger (EXP. 2 in Table 1). The O_3 inlet and outlet concentrations were approximately constant with increasing RH (Figure 6a), indicating that RH did not significantly change O_3 levels in the flow tube. This also shows that the reactivity of the limonene with ozone does not change with RH. The number concentration of the generated particles decreased from 4.9×10^6 cm^{-3} to 2.7×10^6 cm^{-3} with increasing RH, while the peak of the number-size distribution increased slightly, due in part to water absorption. When RH was above 80%, both the integrated number and mass concentrations, which were calculated from the number-size distributions, decreased (Figure 6b).

Despite the change in particle number and mass concentrations with RH, the concentration of all the main HOMs, including RO_2, monomers and dimers, did not change for both OH- and O_3-derived products (Figure 6c). In fact, the only signals in the mass spectra that changed with RH corresponded to an increases associated with water clusters. The variations in HOM concentrations can be explained by the competition between production and condensational losses. As almost all of the detected HOMs are ELVOCs or LVOCs (see Section 3.6), they are not likely to partition back to the gas phase after they encounter a surface. The condensation sink (CS) and wall loss rate for a compound with diffusion coefficient of 8.5×10^{-6} m^2 s^{-1} (e.g., sulfuric acid) were estimated using established methods (Kürten et al., 2014; Crump and Seinfeld, 1981; Kulmala et al., 2001). The calculated CS varied between 0.1-3.5 s^{-1} in different SOA generation experiments, much larger than the wall loss rate (< 0.01 s^{-1}). There was about 5-30% variation in CS in each SOA generation experiment from RH = 3% to 92%. This amount of variation in CS does not seem to have a noticeable influence on the final concentration of HOMs. To further test the hypothesis that variations in condensation sink do not impact final HOM concentrations, particle free experiments were performed and, again, detected HOM concentrations did not change with RH (Figure 7).

3.4 RH influence on SOA generation

Figure 8 shows the integrated SOA particle number and mass concentrations over the observed diameter range of 10 - 100

nm. The generated SOA particle number and mass concentrations for limonene (2.2-6.0 × 10^6 cm^{-3} for number concentrations and 470-1025 μg m^{-3} for mass concentrations) were ~3-12 times greater than for Δ^3-carene (0.3-2.0 × 10^6 cm^{-3} for number concentrations and 56-86 μg m^{-3} for mass concentrations) and α-pinene (0.4-2.2 × 10^6 cm^{-3} for number concentrations and 61-130 μg m^{-3} for mass concentrations). This is because the theoretical ozone reactivity of limonene is 3~5 times higher than the latter two and molar yield from limonene ozonolysis is also the highest. Peaks in the particle number-size distributions were between 40 and 70 nm (Figure S5). In most of the experiments, generated SOA mass concentrations increased or decreased slightly when RH increased from ~0% to ~60% and decreased as RH further increased to ~90%. The variability in particle mass concentration as a function of RH for different experiments can be attributed to combined effects of gas phase reactions, condensed phase reactions, physical uptake of water, as well as the re-evaporation of semi-volatile compounds from the wall. We cannot accurately quantify these effects. As a result, although the measured SOA mass concentration remained relatively constant, we cannot draw conclusions from this observation. In contrast, while particle number concentrations may also be affected by the factors mentioned above, they decreased by a factor of 2~3 with increasing RH.

A number of studies have demonstrated different water and OH influences on the ozonolysis products of exocyclic and endocyclic organic compounds. They have reported either suppressing (Bonn et al., 2002; Bonn and Moorgat, 2002) or promoting (Jonsson et al., 2006; Jonsson et al., 2008) effects of water vapor on the particle formation processes during ozonolysis of monoterpenes by measuring the number-size distributions of generated SOA particles with SMPS. The discrepancies between different results could be attributed to the different experiment setups, e.g., monoterpene and O_3 concentration, temperature, RH range, OH scavengers, reaction time, and so on. Specifically, our results are in good agreement with those of Bonn et al., who studied SOA generation from the ozonolysis of endocyclic monoterpenes (Bonn et al., 2002). In that study, SOA number concentrations decreased by a factor of 1.1~2.5 as RH increased, while the variation in volume concentrations was negligible (within ±10%). They concluded that water's influence on non-volatile products, which are responsible for the initial steps of nucleation, was much larger than its influence for semi-volatile compounds which mainly determined the final volume concentrations of particles. Thus, it was highly suspected that water influenced new particle formation through influencing the generation of NPF precursors. However, our measurements indicate that at least the formation of the detected HOMs is independent of water vapor concentrations. There may be other species that are crucial to the initial steps of NPF and are affected by water vapor but are not detected by nitrate CIMS (see section 3.5). Another possible explanation is that a fraction of HOMs cluster with water at high RH in such a way that they may no longer be able to participate in further cluster formation, thereby suppressing NPF. If the CIMS measurement only detected the declustered molecule, then such a mechanism may still be consistent with our observations.

3.5 Possible formation pathways of water-relevant C_{10} and C_{20} HOMs

Although the oxidation of BVOCs has been widely studied, it has mostly been constrained to the early stages (first and second generation intermediates) and many uncertainties still exist (Johnson and Marston, 2008; Isaacman-VanWertz et al., 2018; Atkinson and Arey, 2003). The first step of ozonolysis for the three BVOCs (α-pinene, $\triangle^3$-carene and limonene) is ozone attack on the endocyclic carbon double bond to form a primary ozonide. Figure 9 shows the O_3-initiated oxidation pathways of α-pinene that may be related to the detected C_{10} and C_{20} HOMs for representative isomers. The primary ozonide rapidly transforms to two excited Criegee intermediates (eCIs), one of which (branching ratio= 0.4) (Kamens et al., 1999) is shown in Figure 9. The reaction pathways of the eCI are complex, the most important two under ambient and most chamber conditions are the sCI channel (reaction I) and the hydroperoxide channel (reaction II) (Bonn et al., 2002). The sCI either reacts with aldehydes to form a secondary ozonide (when the aldehyde is C_{10}, then the formed SOZ is C_{20} and is marked as sCI-C_{10}) or with water or other acidic compounds such as alcohols and carboxylic acids to form hydroxy-hydroperoxide, which then decomposes to carboxylic acids or aldehydes. For α-pinene, the main decomposition product is pinonic acid. In the hydroperoxide channel (reaction II), the formed hydroperoxide quickly decomposes to a first generation alkyl radical (R) and OH (Johnson and Marston, 2008). R reacts with O_2 immediately to form the first generation RO_2, which can undergo numerous reactions, including reaction with HO_2, $R'O_2$ and autoxidation. The reaction with HO_2 mainly forms hydroperoxides, with a small fraction forming hydroxyl or carbonyl-containing compounds. When reacted with another $R'O_2$, either ROOR' or an alkoxy radical (RO) or a carbonyl and a hydroxyl are formed. The RO can undergo isomerization, or form a carbonyl and HO_2, for which the branching ratios are extremely difficult to evaluate. RO can also undergo decomposition, which is one of the pathways to form C_5~C_9. The autoxidation process is key to HOM formation. Each autoxidation step adds two O atoms to the molecule and thus increases the oxidation state very rapidly. The competition between autoxidation processes and bimolecular reactions (RO_2 reactions with $R'O_2$ or HO_2) determines the ultimate oxidation state of the products (Barsanti et al., 2017; Crounse et al., 2013; Rissanen et al., 2015).

OH can be generated in the ozonolysis of alkenes and the yield is near unity (Atkinson, 1997). The reaction of OH with α-pinene directly forms first generation R and then RO_2; one possible structure for this RO_2 (branching ratio = 0.44), formed from OH addition to the double bond (Berndt et al., 2016), is shown in Figure 9. However, the formed RO_2 ($C_{10}H_{17}O_{2m+1}$) are not the same RO_2 as those formed through ozonolysis ($C_{10}H_{15}O_{2n+2}$) (McVay et al., 2016). Accordingly, the structure and composition of C_{10} and C_{20} HOMs formed from OH or O_3 chemistry are different, and so too are their potential impacts on NPF. The combined OH- and O_3-derived dimers ($C_{10}H_{32}O_{2(m+n)+3}$), formed by collision of an OH-derived RO_2 with an

O_3-derived RO_2, were only observed in ozonolysis experiments without OH scavenger.

The RO_2 autoxidation pathway explains most of the observed C_{10} and C_{20} compounds in the mass spectra. One exception to this is that $C_{10}H_{18}O_{2m+1}$, $C_{10}H_{18}O_{2m}$ and $C_{20}H_{34}O_{2(m+m')}$ were not observed in the spectrum whereas in experiments performed by Berndt et al., in which OH oxidation for α-pinene was studied, $C_{10}H_{18}O_{2m}$ and $C_{20}H_{34}O_{2(m+m')}$ dominated the mass spectrum (Berndt et al., 2016). This could be explained by a lower OH/O_3 ratio in our experiments, since unlike Berndt et al. we did not provide an extra source of OH to the flow tube. Also, Berndt and coauthors reported lower sensitivity of nitrate reagent ions to OH-related RO2 compared to other reagent ions such as acetate.

Despite this close agreement achieved by the RO_2 autoxidation mechanism and the observed mass spectra in our study, prior studies suggest that other potential pathways cannot be excluded. An accretion product involving sCI is one possibility (Barsanti et al., 2017). It is possible that sCI reacts with long-chain carboxylic acids or carbonyls, such as those with 10 carbon atoms, forming in this instance anhydrides (sCI-C_{10}, reaction IV) or secondary ozonides (sCI-C_{10}, reaction V) with vapor pressures lower than 10^{-15} torr (Kamens et al., 1999; Tobias and Ziemann, 2001; Bonn et al., 2002). The formation of anhydride is more likely in condensed phase, whereas there is also a possibility it can also happen in gas phase (Kamens et al., 1999). However, it is unknown whether these sCI-C_{10} can be detected using nitrate-CIMS as they may lack hydrogen bond donor moieties. The semi-volatile pinonic acid can also form HOMs after further oxidation by OH (Ehn et al., 2014), provided that excess α-pinene is not present to compete with pinonic acid for the generated OH.

Water vapor's influence on HOM formation can be direct or indirect. For monoterpene oxidation, the direct participation of water vapor is to react with sCI, favoring the formation of the hydroperoxide and its decomposition products (reaction III) over the secondary ozonides (sCI-C_{10}, reaction IV) or possible anhydrides (sCI-C_{10}, reaction V). Since the formation of sCI-C_{10} is more likely to contribute to NPF than the products from sCI and water vapor (Kamens et al., 1999; Tobias et al., 2000), a decrease in low volatility sCI-C_{10} with high RH could explain the decreasing SOA number concentrations in our experiment. It has been shown previously that OH yields from the reactions of O_3 with a series of monoterpenes were not affected by the presence of water vapor (Atkinson et al., 1992; Aschmann et al., 2002), which implies that the hydroperoxide channel (reaction II) are similarly unaffected by water. Since the detected HOMs in our experiments were RH-independent, we conclude that all the detected HOMs were formed from hydroperoxide channel (reaction II) and not via the sCI channel (reaction I). Similarly, the detected HOMs were not likely to form through the hydration reaction (Equation 1) (Ehn et al., 2012), which is supposed to increase with increasing RH.

359 $$R-CHO + H_2O \rightarrow R-CH(OH)_2 \quad .$$ (Equation 1)

360

361 The indirect water effect on HOM formation includes the water influence on HO_2 fate. As water promotes HO_2 self-reaction
362 (Equation 2), reaction of HO_2 with RO_2 should decrease and the related HOM monomers should likewise decrease with
363 increasing RH. However, as the formation of both HOM monomers and dimers was not affected by H_2O, it was likely that
364 water does not significantly increase HO_2 self-reaction or that HO_2 chemistry was not important in our experiments.

365 $$2HO_2 \xrightarrow{M, H_2O} H_2O_2 + O_2$$ (Equation 2)

366

367 **3.6 Volatility predictions**

368 The volatility of the gas phase products is one of the most important properties that determines whether a compound
369 contributes to the formation, initial growth or further growth of SOA particles (Donahue et al., 2012; Kroll et al., 2011). As
370 the products with identical elemental composition can be formed from different bimolecular reactions of the intermediate
371 RO_2, it is difficult to predict their exact structures. For the current study, the number of different structural and functional
372 groups (e.g., aromatic rings, aldehydes, ketones, hydroxyls, peroxides, hydro-peroxides) was estimated and used to derive
373 saturation vapor pressure using SIMPOL.1 (Table S1). To simplify the calculation, the functional groups used here were
374 directly predicted from the proposed formation pathways in Figure 10 and did not include intramolecular isomerization,
375 although that may be important in some situations. For example, one of the ROOH can be replaced with an endo-peroxide
376 via ring closure of unsaturated RO_2 (Berndt et al., 2016). It has to be noted that the group contribution methods very likely
377 underestimate the volatility of HOM product from α-pinene autoxidation products due to ignoring intramolecular H-bonding
378 (Kurtén et al., 2016). There may be large uncertainties in SIMPOL method as well as in our functional group estimation
379 process. As a comparison, the Molecular Corridor method (Li et al., 2016), which does not require information on functional
380 groups, was used to estimate the saturation vapor pressure as well. The average carbon oxidation state ($\overline{OS}_C$) was calculated
381 with Equation 3, in replacement of the commonly used formula ($\overline{OS}_C = 2O:C - H:C$), as the second oxygen atom in (hydro)
382 peroxide group does not increase the carbon oxidation state. In equation 3, n_O, n_C, and n_H are the oxygen, carbon, and
383 hydrogen numbers in the molecule; $n_{(hydro)peroxide}$ is the number of (hydro) peroxide groups in the molecule.

384 $$\overline{OS}_C = \frac{2n_O - n_{(hydro)peroxide} - n_H}{n_C}$$ (Equation 3)

385 Figure 10 shows the predicted saturation mass concentrations (C*) of the main C_{10} and C_{20} closed shell products. The
386 difference of C* predicted from the two methods was ~1-4 orders of magnitudes. Despite these differences, most of the C_{20}
387 HOMs can be classified as ELVOCs, while C_{10} products were mostly LVOCs. Typically, t for those compounds with

identical $\overline{OSc}$, such as $C_{20}H_{30}O_{10}$ (O_3-derived dimer, $\log_{10}(C^*)$=-2.74), $C_{20}H_{32}O_{11}$ (OH and O_3 combined dimer, $\log_{10}(C^*)$=-5.11), $C_{20}H_{34}O_{12}$ (OH-derived dimer, $\log_{10}(C^*)$=-7.41), OH-derived HOMs have lower volatilities than O_3-derived HOMs due to a greater number of (hydro) peroxide groups.

4 Conclusions

The RH influence on HOM formation and NPF during monoterpene oxidation was explored in this study. HOMs were detected with a TI-CIMS, using nitrate as reagent ions; C_{10} and C_{20} dominated the spectra. There are mainly three potential paths for water vapor influence on the formation of C_{10} and C_{20} HOMs. One is water reacting with sCI (Equation 1), thereby influencing the branching ratio between formation of more volatile compounds decomposed from hydroxyl hydroperoxide, such as pinonic acid, and accretion products with sCI such as secondary ozonide (sCI-C_{10}) and anhydride (sCI-C_{10}). The second hypothesized water influence is on the HOMs formed from hydration reactions (Equation 2). The third is that water increases the rate of self-reaction of HO_2 (Equation 3), thus indirectly impacts the loss pathways of RO_2. Our experimental results, both with high particle loading and particle-free conditions, demonstrated that neither the detected HOM species nor their signal abundance changed significantly with RH. This indicates that the detected HOMs, which can mostly be explained by RO_2 autoxidation, must be formed from water-independent pathways rather than by those reactions mentioned above. One implication of this result is that HO_2 self-reaction was not significantly promoted by water or that the RO_2 reaction with HO_2 was not be significant in our system, but instead that RO_2 reacts with another peroxy radical, R'O_2, to generate both closed shell monomers and dimers. Another implication is that the sCI pathway is not responsible for the generation of the detected HOMs while the role of sCI-related HOMs (SOZ or anhydride) formation by accretion with long chain products, which may not be detected with nitrate CIMS, may be important in causing the decrease in SOA number concentrations with increased RH. Another possible explanation for the decreasing SOA number concentration is that water may cluster with HOMs and suppress NPF.

The detected HOMs, which could mostly be explained by autoxidation of RO_2 followed by reactions with R'O_2 or HO_2, were distinguished as OH-related, O_3-related RO_2, closed shell HOM monomers, and HOM dimers. The volatility of the identified products were estimated with the SIMPOL.1 group contribution method and with the molecular corridor technique. That analysis confirmed that C_{20} closed shell products have significantly lower volatility compared to C_{10} products and are thus more likely to contribute to NPF. For the HOM products with identical $\overline{OSc}$, OH-derived HOMs have lower volatilities than O_3-derived HOMs due to a greater number of (hydro) peroxide groups. As a result, OH chemistry is suspected to be more

likely to lead to NPF than O_3 chemistry, given the same level of oxidants and VOCs precursors.

Acknowledgements

This research was supported by the US Department of Energy's Atmospheric System Research program under grant no. DESC0014469, the US National Science Foundation under grant no. AGS-1762098, and by the National Key R&D Program of China under grant no. 2017YFC0209503. XL thanks the financial support from the State Scholarship Fund managed by Chinese Scholarship Council (CSC). We thank Hayley Glicker, Deanna Caroline Myers, Michael Lawler, and Danielle Draper for their kind help.

References

Andreae, M. O., Afchine, A., Albrecht, R., Holanda, B. A., Artaxo, P., Barbosa, H. M., Borrmann, S., Cecchini, M. A., Costa, A., and Dollner, M.: Aerosol characteristics and particle production in the upper troposphere over the Amazon Basin, Atmos Chem Phys, 18, 921-961, 2018.

Aschmann, S. M., Arey, J., and Atkinson, R.: OH radical formation from the gas-phase reactions of O-3 with a series of terpenes, Atmos Environ, 36, 4347-4355, 10.1016/s1352-2310(02)00355-2, 2002.

Atkinson, R., Aschmann, S. M., Arey, J., and Shorees, B.: Formation of OH radicals in the gas phase reactions of O3 with a series of terpenes, Journal of Geophysical Research: Atmospheres, 97, 6065-6073, 1992.

Atkinson, R.: Gas-phase tropospheric chemistry of volatile organic compounds: 1. Alkanes and alkenes, Journal of Physical and Chemical Reference Data, 26, 215-290, 1997.

Atkinson, R., and Arey, J.: Gas-phase tropospheric chemistry of biogenic volatile organic compounds: a review, Atmos Environ, 37, 197-219, 2003.

Ball, S. M., Hanson, D. R., Eisele, F. L., and McMurry, P. H.: Laboratory studies of particle nucleation: Initial results for H2SO4, H2O, and NH3 vapors, J Geophys Res-Atmos, 104, 23709-23718, 10.1029/1999jd900411, 1999.

Barsanti, K. C., Kroll, J. H., and Thornton, J. A.: Formation of Low-Volatility Organic Compounds in the Atmosphere: Recent Advancements and Insights, Journal of Physical Chemistry Letters, 8, 1503-1511, 10.1021/acs.jpclett.7b02969, 2017.

Berndt, T., Richters, S., Jokinen, T., Hyttinen, N., Kurtén, T., Otkjær, R. V., Kjaergaard, H. G., Stratmann, F., Herrmann, H., and Sipilä, M.: Hydroxyl radical-induced formation of highly oxidized organic compounds, Nature communications, 7, 13677, 2016.

Bianchi, F., Tröstl, J., Junninen, H., Frege, C., Henne, S., Hoyle, C. R., Molteni, U., Herrmann, E., Adamov, A., and Bukowiecki, N.: New particle formation in the free troposphere: A question of chemistry and timing, Science, aad5456, 2016.

Bonn, B., and Moorgat, G.: New particle formation during a-and b-pinene oxidation by O 3, OH and NO 3, and the influence of water vapour: particle size distribution studies, Atmos Chem Phys, 2, 183-196, 2002.

Bonn, B., Schuster, G., and Moortgat, G. K.: Influence of water vapor on the process of new particle formation during monoterpene ozonolysis, The Journal of Physical Chemistry A, 106, 2869-2881, 2002.

Boy, M., and Kulmala, M.: Nucleation events in the continental boundary layer: Influence of physical and meteorological parameters, Atmos Chem Phys, 2, 1-16, 2002.

Burkholder, J. B., Baynard, T., Ravishankara, A. R., and Lovejoy, E. R.: Particle nucleation following the O-3 and OH initiated oxidation of alpha-pinene and beta-pinene between 278 and 320 K, J Geophys Res-Atmos, 112, 10.1029/2006jd007783, 2007.

Cai, R., Yang, D., Fu, Y., Wang, X., Li, X., Ma, Y., Hao, J., Zheng, J., and Jiang, J.: Aerosol surface area concentration: a governing factor in new particle formation in Beijing, Atmos Chem Phys, 17, 12327, 2017.

Chen, H., Ezell, M. J., Arquero, K. D., Varner, M. E., Dawson, M. L., Gerber, R. B., and Finlayson-Pitts, B. J.: New particle formation and growth from methanesulfonic acid, trimethylamine and water, Physical Chemistry Chemical Physics, 17, 13699-13709, 2015.

Chen, M., Titcombe, M., Jiang, J., Jen, C., Kuang, C., Fischer, M. L., Eisele, F. L., Siepmann, J. I., Hanson, D. R., and Zhao, J.: Acid–base chemical reaction model for nucleation rates in the polluted atmospheric boundary layer, Proceedings of the National Academy of Sciences, 109, 18713-18718, 2012.

Crounse, J. D., Nielsen, L. B., Jørgensen, S., Kjaergaard, H. G., and Wennberg, P. O.: Autoxidation of organic compounds in the atmosphere, The Journal of Physical Chemistry Letters, 4, 3513-3520, 2013.

Crump, J. G., and Seinfeld, J. H.: TURBULENT DEPOSITION AND GRAVITATIONAL SEDIMENTATION OF AN AEROSOL IN A VESSEL OF ARBITRARY SHAPE, J Aerosol Sci, 12, 405-415, 10.1016/0021-8502(81)90036-7, 1981.

Dada, L., Paasonen, P., Nieminen, T., Buenrostro Mazon, S., Kontkanen, J., Peräkylä, O., Lehtipalo, K., Hussein, T., Petäjä, T., and Kerminen, V.-M.: Long-term analysis of clear-sky new particle formation events and nonevents in Hyytiälä, Atmos Chem Phys, 17, 6227-6241, 2017.

Donahue, N. M., Trump, E. R., Pierce, J. R., and Riipinen, I.: Theoretical constraints on pure vapor-pressure driven condensation of organics to ultrafine particles, Geophys Res Lett, 38, 10.1029/2011gl048115, 2011.

Donahue, N. M., Kroll, J., Pandis, S. N., and Robinson, A. L.: A two-dimensional volatility basis set–Part 2: Diagnostics of organic-aerosol evolution, Atmos Chem Phys, 12, 615-634, 2012.

Donahue, N. M., Ortega, I. K., Chuang, W., Riipinen, I., Riccobono, F., Schobesberger, S., Dommen, J., Baltensperger, U., Kulmala, M., Worsnop, D. R., and Vehkamaki, H.: How do organic vapors contribute to new-particle formation?, Faraday discussions, 165, 91-104, 10.1039/c3fd00046j, 2013.

Dunne, E. M., Gordon, H., Kürten, A., Almeida, J., Duplissy, J., Williamson, C., Ortega, I. K., Pringle, K. J., Adamov, A., Baltensperger, U., Barmet, P., Benduhn, F., Bianchi, F., Breitenlechner, M., Clarke, A., Curtius, J., Dommen, J., Donahue, N. M., Ehrhart, S., Flagan, R. C., Franchin, A., Guida, R., Hakala, J., Hansel, A., Heinritzi, M., Jokinen, T., Kangasluoma, J., Kirkby, J., Kulmala, M., Kupc, A., Lawler, M. J., Lehtipalo, K., Makhmutov, V., Mann, G., Mathot, S., Merikanto, J., Miettinen, P., Nenes, A., Onnela, A., Rap, A., Reddington, C. L. S., Riccobono, F., Richards, N. A. D., Rissanen, M. P., Rondo, L., Sarnela, N., Schobesberger, S., Sengupta, K., Simon, M., Sipila, M., Smith, J. N., Stozkhov, Y., Tome, A., Trostl, J., Wagner, P. E., Wimmer, D., Winkler, P. M., Worsnop, D. R., and Carslaw, K. S.: Global atmospheric particle formation from CERN CLOUD measurements, Science, 354, 1119-1124, 10.1126/science.aaf2649, 2016.

Duplissy, J., Merikanto, J., Franchin, A., Tsagkogeorgas, G., Kangasluoma, J., Wimmer, D., Vuollekoski, H., Schobesberger, S., Lehtipalo, K., and Flagan, R.: Effect of ions on sulfuric acid - water binary particle formation: 2. Experimental data and comparison with QC - normalized classical nucleation theory, Journal of Geophysical Research: Atmospheres, 121, 1752-1775, 2016.

Ehn, M., Kleist, E., Junninen, H., Petäjä, T., Lönn, G., Schobesberger, S., Maso, M. D., Trimborn, A., Kulmala, M., and Worsnop, D.: Gas phase formation of extremely oxidized pinene reaction products in chamber and ambient air, Atmos Chem Phys, 12, 5113-5127, 2012.

Ehn, M., Thornton, J. A., Kleist, E., Sipila, M., Junninen, H., Pullinen, I., Springer, M., Rubach, F., Tillmann, R., Lee, B., Lopez-Hilfiker, F., Andres, S., Acir, I.-H., Rissanen, M., Jokinen, T., Schobesberger, S., Kangasluoma, J., Kontkanen, J., Nieminen, T., Kurtén, T., Nielsen, L. B., Jorgensen, S., Kjaergaard, H. G., Canagaratna, M., Dal Maso, M., Berndt, T., Petaja, T., Wahner, A., Kerminen, V.-M., Kulmala, M., Worsnop, D. R., Wildt, J., and Mentel, T. F.: A large source of low-volatility secondary organic aerosol, Nature, 506, 476-+, 10.1038/nature13032, 2014.

Eisele, F. L., and Tanner, D. J.: Measurement of the gas-phas concentration of H2SO4 and methane sulfonic-acid and estimates of H2SO4 production and loss in the atmosphere, J Geophys Res-Atmos, 98, 9001-9010, 10.1029/93jd00031, 1993.

Frege, C., Ortega, I. K., Rissanen, M. P., Praplan, A. P., Steiner, G., Heinritzi, M., Ahonen, L., Amorim, A., Bernhammer, A.-K., and Bianchi, F.: Influence of temperature on the molecular composition of ions and charged clusters during pure biogenic nucleation, Atmos Chem Phys, 18, 65-79, 2018.

Hamed, A., Korhonen, H., Sihto, S. L., Joutsensaari, J., Järvinen, H., Petäjä, T., Arnold, F., Nieminen, T., Kulmala, M., and Smith, J. N.: The role of relative humidity in continental new particle formation, Journal of Geophysical Research: Atmospheres, 116, 2011.

Hanson, D., McMurry, P., Jiang, J., Tanner, D., and Huey, L.: Ambient pressure proton transfer mass spectrometry: detection of amines and ammonia, Environ Sci Technol, 45, 8881-8888, 2011.

Hoffmann, T., O'Dowd, C. D., and Seinfeld, J. H.: Iodine oxide homogeneous nucleation: An explanation for coastal new particle production, Geophys Res Lett, 28, 1949-1952, 2001.

Hyttinen, N., Kupiainen-Määttä, O., Rissanen, M. P., Muuronen, M., Ehn, M., and Kurtén, T.: Modeling the charging of highly oxidized cyclohexene ozonolysis products using nitrate-based chemical ionization, The Journal of Physical Chemistry A, 119, 6339-6345, 2015.

Hyvönen, S., Junninen, H., Laakso, L., Maso, M. D., Grönholm, T., Bonn, B., Keronen, P., Aalto, P., Hiltunen, V., and Pohja, T.: A look at aerosol formation using data mining techniques, Atmos Chem Phys, 5, 3345-3356, 2005.

Isaacman-VanWertz, G., Massoli, P., O'Brien, R., Lim, C., Franklin, J. P., Moss, J. A., Hunter, J. F., Nowak, J. B., Canagaratna, M. R., and Misztal, P. K.: Chemical evolution of atmospheric organic carbon over multiple generations of oxidation, Nature chemistry, 1, 2018.

Johnson, D., and Marston, G.: The gas-phase ozonolysis of unsaturated volatile organic compounds in the troposphere, Chemical Society Reviews, 37, 699-716, 2008.

Jokinen, T., Sipila, M., Junninen, H., Ehn, M., Lonn, G., Hakala, J., Petaja, T., Mauldin, R. L., Kulmala, M., and Worsnop, D. R.: Atmospheric sulphuric acid and neutral cluster measurements using CI-APi-TOF, Atmos Chem Phys, 12, 4117-4125, 2012.

Jokinen, T., Sipilä, M., Richters, S., Kerminen, V. M., Paasonen, P., Stratmann, F., Worsnop, D., Kulmala, M., Ehn, M., and Herrmann, H.: Rapid autoxidation forms highly oxidized RO2 radicals in the atmosphere, Angewandte Chemie International Edition, 53, 14596-14600, 2014.

Jonsson, Å. M., Hallquist, M., and Ljungström, E.: Impact of humidity on the ozone initiated oxidation of limonene, Δ3-carene, and α-pinene, Environ Sci Technol, 40, 188-194, 2006.

Jonsson, Å. M., Hallquist, M., and Ljungström, E.: Influence of OH scavenger on the water effect on secondary organic aerosol formation from ozonolysis of limonene, Δ3-carene, and α-pinene, Environ Sci Technol, 42, 5938-5944, 2008.

Junninen, H., Ehn, M., Petaja, T., Luosujarvi, L., Kotiaho, T., Kostiainen, R., Rohner, U., Gonin, M., Fuhrer, K., Kulmala, M., and Worsnop, D. R.: A high-resolution mass spectrometer to measure atmospheric ion composition, Atmos Meas Tech, 3, 1039-1053, 2010.

Kamens, R., Jang, M., Chien, C.-J., and Leach, K.: Aerosol Formation from the Reaction of α-Pinene and Ozone Using a Gas-Phase Kinetics-Aerosol Partitioning Model, Environ Sci Technol, 33, 1430-1438, 10.1021/es980725r, 1999.

Kroll, J. H., Donahue, N. M., Jimenez, J. L., Kessler, S. H., Canagaratna, M. R., Wilson, K. R., Altieri, K. E., Mazzoleni, L. R., Wozniak, A. S., Bluhm, H., Mysak, E. R., Smith, J. D., Kolb, C. E., and Worsnop, D. R.: Carbon oxidation state as a metric for describing the chemistry of atmospheric organic aerosol, Nature Chemistry, 3, 133-139, 10.1038/nchem.948, 2011.

Kuang, C., McMurry, P. H., McCormick, A. V., and Eisele, F. L.: Dependence of nucleation rates on sulfuric acid vapor concentration in diverse atmospheric locations, J Geophys Res, 113, 10.1029/2007jd009253, 2008.

Kulmala, M., Dal Maso, M., Makela, J. M., Pirjola, L., Vakeva, M., Aalto, P., Miikkulainen, P., Hameri, K., and O'Dowd, C.

D.: On the formation, growth and composition of nucleation mode particles, Tellus B, 53, 479-490, 10.1034/j.1600-0889.2001.d01-33.x, 2001.

Kulmala, M., Vehkamäki, H., Petäjä, T., Dal Maso, M., Lauri, A., Kerminen, V. M., Birmili, W., and McMurry, P. H.: Formation and growth rates of ultrafine atmospheric particles: a review of observations, J Aerosol Sci, 35, 143-176, 10.1016/j.jaerosci.2003.10.003, 2004.

Kulmala, M., Petäjä, T., Ehn, M., Thornton, J., Sipilä, M., Worsnop, D., and Kerminen, V.-M.: Chemistry of atmospheric nucleation: on the recent advances on precursor characterization and atmospheric cluster composition in connection with atmospheric new particle formation, Annual review of physical chemistry, 65, 21-37, 2014.

Kürten, A., Rondo, L., Ehrhart, S., and Curtius, J.: Calibration of a Chemical Ionization Mass Spectrometer for the Measurement of Gaseous Sulfuric Acid, J Phys Chem A, 116, 6375-6386, 2012.

Kürten, A., Jokinen, T., Simon, M., Sipila, M., Sarnela, N., Junninen, H., Adamov, A., Almeida, J., Amorim, A., Bianchi, F., Breitenlechner, M., Dommen, J., Donahue, N. M., Duplissy, J., Ehrhart, S., Flagan, R. C., Franchin, A., Hakala, J., Hansel, A., Heinritzi, M., Hutterli, M., Kangasluoma, J., Kirkby, J., Laaksonen, A., Lehtipalo, K., Leiminger, M., Makhmutov, V., Mathot, S., Onnela, A., Petaja, T., Praplan, A. P., Riccobono, F., Rissanen, M. P., Rondo, L., Schobesberger, S., Seinfeld, J. H., Steiner, G., Tome, A., Troestl, J., Winkler, P. M., Williamson, C., Wimmer, D., Ye, P., Baltensperger, U., Carslaw, K. S., Kulmala, M., Worsnop, D. R., and Curtius, J.: Neutral molecular cluster formation of sulfuric acid-dimethylamine observed in real time under atmospheric conditions, P Natl Acad Sci USA, 111, 15019-15024, 10.1073/pnas.1404853111, 2014.

Kürten, A., Bergen, A., Heinritzi, M., Leiminger, M., Lorenz, V., Piel, F., Simon, M., Sitals, R., Wagner, A. C., and Curtius, J.: Observation of new particle formation and measurement of sulfuric acid, ammonia, amines and highly oxidized organic molecules at a rural site in central Germany, Atmos Chem Phys, 16, 12793-12813, 10.5194/acp-16-12793-2016, 2016.

Kurten, T., Rissanen, M. P., Mackeprang, K., Thornton, J. A., Hyttinen, N., Jorgensen, S., Ehn, M., and Kjaergaard, H. G.: Computational Study of Hydrogen Shifts and Ring-Opening Mechanisms in alpha-Pinene Ozonolysis Products, J Phys Chem A, 119, 11366-11375, 10.1021/acs.jpca.5b08948, 2015.

Kurtén, T., Tiusanen, K., Roldin, P., Rissanen, M., Luy, J.-N., Boy, M., Ehn, M., and Donahue, N.: α-Pinene Autoxidation Products May Not Have Extremely Low Saturation Vapor Pressures Despite High O:C Ratios, The Journal of Physical Chemistry A, 120, 2569-2582, 10.1021/acs.jpca.6b02196, 2016.

Lee, B. H., Lopez-Hilfiker, F. D., Mohr, C., Kurtén, T., Worsnop, D. R., and Thornton, J. A.: An iodide-adduct high-resolution time-of-flight chemical-ionization mass spectrometer: Application to atmospheric inorganic and organic compounds, Environ Sci Technol, 48, 6309-6317, 2014.

Li, Y., Poeschl, U., and Shiraiwa, M.: Molecular corridors and parameterizations of volatility in the chemical evolution of organic aerosols, Atmos Chem Phys, 16, 3327-3344, 10.5194/acp-16-3327-2016, 2016.

Makkonen, R., Asmi, A., Kerminen, V. M., Boy, M., Arneth, A., Hari, P., and Kulmala, M.: Air pollution control and decreasing new particle formation lead to strong climate warming, Atmos Chem Phys, 12, 1515-1524, 10.5194/acp-12-1515-2012, 2012.

McVay, R. C., Zhang, X., Aumont, B., Valorso, R., Camredon, M., La, Y. S., Wennberg, P. O., and Seinfeld, J. H.: SOA formation from the photooxidation of α-pinene: systematic exploration of the simulation of chamber data, Atmos Chem Phys, 16, 2785-2802, 2016.

Merikanto, J., Spracklen, D., Mann, G., Pickering, S., and Carslaw, K.: Impact of nucleation on global CCN, Atmos Chem Phys, 9, 8601-8616, 2009.

Merikanto, J., Duplissy, J., Määttänen, A., Henschel, H., Donahue, N. M., Brus, D., Schobesberger, S., Kulmala, M., and Vehkamäki, H.: Effect of ions on sulfuric acid - water binary particle formation: 1. Theory for kinetic - and nucleation - type particle formation and atmospheric implications, Journal of Geophysical Research: Atmospheres, 121, 1736-1751, 2016.

Metzger, A., Verheggen, B., Dommen, J., Duplissy, J., Prevot, A. S., Weingartner, E., Riipinen, I., Kulmala, M., Spracklen, D. V., Carslaw, K. S., and Baltensperger, U.: Evidence for the role of organics in aerosol particle formation under atmospheric

conditions, Proc Natl Acad Sci U S A, 107, 6646-6651, 10.1073/pnas.0911330107, 2010.
Molteni, U., Bianchi, F., Klein, F., Haddad, I. E., Frege, C., Rossi, M. J., Dommen, J., and Baltensperger, U.: Formation of highly oxygenated organic molecules from aromatic compounds, Atmos Chem Phys, 18, 1909-1921, 2018.
Napari, I., Noppel, M., Vehkamäki, H., and Kulmala, M.: Parametrization of ternary nucleation rates for H2SO4 - NH3 - H2O vapors, Journal of Geophysical Research: Atmospheres, 107, 2002.
O'Dowd, C. D., Geever, M., Hill, M. K., Smith, M. H., and Jennings, S. G.: New particle formation: Nucleation rates and spatial scales in the clean marine coastal environment, Geophys Res Lett, 25, 1661-1664, 1998.
Ortega, I. K., Donahue, N. M., Kurtén, T., Kulmala, M., Focsa, C., and Vehkamaki, H.: Can Highly Oxidized Organics Contribute to Atmospheric New Particle Formation?, J Phys Chem A, 120, 1452-1458, 10.1021/acs.jpca.5b07427, 2016.
Pankow, J. F., and Asher, W. E.: SIMPOL. 1: a simple group contribution method for predicting vapor pressures and enthalpies of vaporization of multifunctional organic compounds, Atmos Chem Phys, 8, 2773-2796, 2008.
Poschl, U., Martin, S. T., Sinha, B., Chen, Q., Gunthe, S. S., Huffman, J. A., Borrmann, S., Farmer, D. K., Garland, R. M., Helas, G., Jimenez, J. L., King, S. M., Manzi, A., Mikhailov, E., Pauliquevis, T., Petters, M. D., Prenni, A. J., Roldin, P., Rose, D., Schneider, J., Su, H., Zorn, S. R., Artaxo, P., and Andreae, M. O.: Rainforest Aerosols as Biogenic Nuclei of Clouds and Precipitation in the Amazon, Science, 329, 1513-1516, 2010.
Rissanen, M. P., Kurtén, T., Sipilä, M., Thornton, J. A., Kausiala, O., Garmash, O., Kjaergaard, H. G., Petäjä, T., Worsnop, D. R., and Ehn, M.: Effects of chemical complexity on the autoxidation mechanisms of endocyclic alkene ozonolysis products: From methylcyclohexenes toward understanding α-pinene, The Journal of Physical Chemistry A, 119, 4633-4650, 2015.
Schobesberger, S., Junninen, H., Bianchi, F., Lonn, G., Ehn, M., Lehtipalo, K., Dommen, J., Ehrhart, S., Ortega, I. K., Franchin, A., Nieminen, T., Riccobono, F., Hutterli, M., Duplissy, J., Almeida, J., Amorim, A., Breitenlechner, M., Downard, A. J., Dunne, E. M., Flagan, R. C., Kajos, M., Keskinen, H., Kirkby, J., Kupc, A., Kürten, A., Kurtén, T., Laaksonen, A., Mathot, S., Onnela, A., Praplan, A. P., Rondo, L., Santos, F. D., Schallhart, S., Schnitzhofer, R., Sipila, M., Tome, A., Tsagkogeorgas, G., Vehkamaki, H., Wimmer, D., Baltensperger, U., Carslaw, K. S., Curtius, J., Hansel, A., Petaja, T., Kulmala, M., Donahue, N. M., and Worsnop, D. R.: Molecular understanding of atmospheric particle formation from sulfuric acid and large oxidized organic molecules, Proc Natl Acad Sci U S A, 110, 17223-17228, 10.1073/pnas.1306973110, 2013.
Shen, X. J., Sun, J. Y., Zhang, Y. M., Wehner, B., Nowak, A., Tuch, T., Zhang, X. C., Wang, T. T., Zhou, H. G., Zhang, X. L., Dong, F., Birmili, W., and Wiedensohler, A.: First long-term study of particle number size distributions and new particle formation events of regional aerosol in the North China Plain, Atmos Chem Phys, 11, 1565-1580, 10.5194/acp-11-1565-2011, 2011.
Sihto, S.-L., Kulmala, M., Kerminen, V.-M., Maso, M. D., Petäjä, T., Riipinen, I., Korhonen, H., Arnold, F., Janson, R., and Boy, M.: Atmospheric sulphuric acid and aerosol formation: implications from atmospheric measurements for nucleation and early growth mechanisms, Atmos Chem Phys, 6, 4079-4091, 2006.
Thomson, B., and Iribarne, J.: Field induced ion evaporation from liquid surfaces at atmospheric pressure, The Journal of Chemical Physics, 71, 4451-4463, 1979.
Tobias, H. J., Docherty, K. S., Beving, D. E., and Ziemann, P. J.: Effect of relative humidity on the chemical composition of secondary organic aerosol formed from reactions of 1-tetradecene and O3, Environ Sci Technol, 34, 2116-2125, 2000.
Tobias, H. J., and Ziemann, P. J.: Kinetics of the gas-phase reactions of alcohols, aldehydes, carboxylic acids, and water with the C13 stabilized Criegee intermediate formed from ozonolysis of 1-tetradecene, The Journal of Physical Chemistry A, 105, 6129-6135, 2001.
Tröstl, J., Chuang, W. K., Gordon, H., Heinritzi, M., Yan, C., Molteni, U., Ahlm, L., Frege, C., Bianchi, F., and Wagner, R.: The role of low-volatility organic compounds in initial particle growth in the atmosphere, Nature, 533, 527-531, 2016.
Vehkamäki, H., and Riipinen, I.: Thermodynamics and kinetics of atmospheric aerosol particle formation and growth, Chemical Society Reviews, 41, 5160-5173, 2012.
Weber, R., Marti, J., McMurry, P., Eisele, F., Tanner, D., and Jefferson, A.: Measurements of new particle formation and ultrafine particle growth rates at a clean continental site, Journal of Geophysical Research: Atmospheres, 102, 4375-4385,

1997.
Weber, R., McMurry, P. H., Mauldin, R., Tanner, D., Eisele, F., Clarke, A., and Kapustin, V.: New particle formation in the remote troposphere: A comparison of observations at various sites, Geophys Res Lett, 26, 307-310, 1999.
Yu, H., McGraw, R., and Lee, S.-H.: Effects of amines on formation of sub-3 nm particles and their subsequent growth, Geophys Res Lett, 39, 10.1029/2011gl050099, 2012.
Zhang, R., Khalizov, A., Wang, L., Hu, M., and Xu, W.: Nucleation and growth of nanoparticles in the atmosphere, Chem Rev, 112, 1957-2011, 10.1021/cr2001756, 2012.
Zhang, X., McVay, R. C., Huang, D. D., Dalleska, N. F., Aumont, B., Flagan, R. C., and Seinfeld, J. H.: Formation and evolution of molecular products in α-pinene secondary organic aerosol, Proceedings of the National Academy of Sciences, 112, 14168-14173, 2015.
Zhao, J., Khalizov, A., Zhang, R., and McGraw, R.: Hydrogen-bonding interaction in molecular complexes and clusters of aerosol nucleation precursors, The Journal of Physical Chemistry A, 113, 680-689, 2009.
Zhao, J., Eisele, F. L., Titcombe, M., Kuang, C., and McMurry, P. H.: Chemical ionization mass spectrometric measurements of atmospheric neutral clusters using the cluster - CIMS, Journal of Geophysical Research: Atmospheres, 115, 2010.
Zhao, J., Ortega, J., Chen, M., and Mcmurry, P. H.: Dependence of particle nucleation and growth on high molecular weight gas phase products during ozonolysis of α-pinene, Atmospheric Chemistry & Physics, 13, 7631-7644, 2013.

651 **Table 1. Experiment conditions and products.**

Precursor	Exp (#)	Monoterpene (ppbv)	O_3 (ppbv)	Cyclo-hexane (ppmv)	Initial rate[1] (10^8 molecules cm^{-3} s^{-1})	O_3 consumption[2] (ppb)	SOA[3] ($\mu g\ m^{-3}$)
Limonene	1	1085	900±10	0	1410	159-166	138-208
	2	1085	900±10	217	1410	139-150	81-147
	3	54	350±5	0	27.3	34-41	0
α-pinene	4	1111	900±10	0	625	103-110	761-1042
	5	1111	900±10	222	625	93-102	414-735
	6	54	350±5	0	11.8	23-30	0
Δ^3-carene	7	1111	900±10	0	267	72-89	55-93
	8	1111	900±10	222	267	70-86	34-92
	9	54	350±5	0	5.05	11-16	0

652 **[1]At room temperature (298K), the rate coefficients for limonene, α-pinene and Δ^3-carene to react with O_3 were 200×10^{-18},**
653 **86.6×10^{-18}, 37×10^{-18} cm^3 $molecule^{-1}$ s^{-1}, respectively.**

654 **[2]O_3 consumption values were calculated from the difference between inlet and outlet O_3 concentrations.**

655 **[3]SOA mass concentrations were calculated from SMPS-measured volume concentrations and an assumed organic effective density**
656 **(1.2 g cm^{-3}).**

657

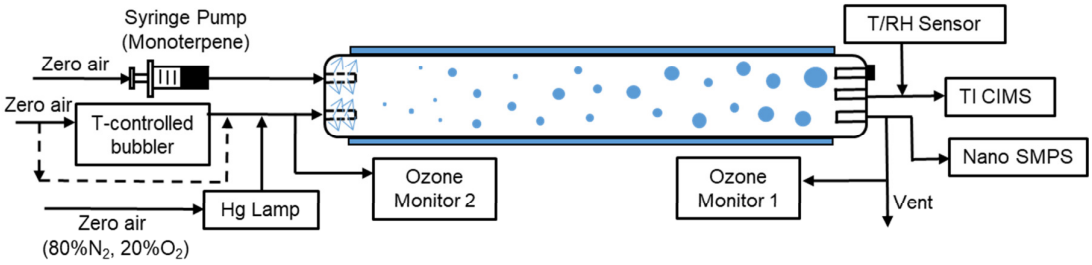

Figure 1. Experiment setup for the flow tube experiments. The 8.5 L flow tube was placed at a temperature-controlled room (21±1°C) and covered. The total flowrate was 8.5 LPM. The RH was adjusted by mixing temperature controlled bubbler flow with dry zero air.

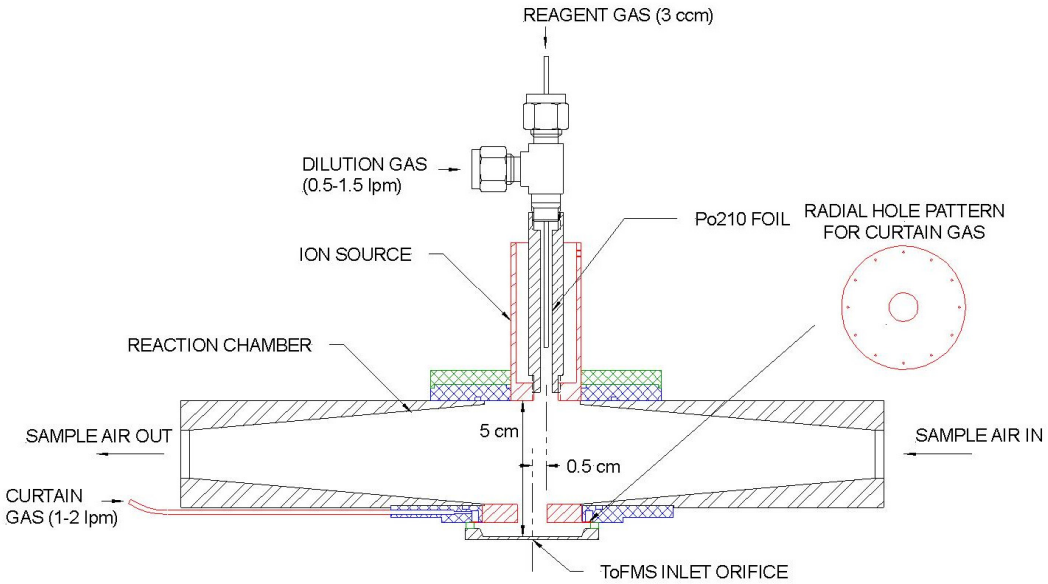

Figure 2. Schematic of the transverse ionization (TI) inlet, showing the N_2 curtain gas configuration. The relative position of the ion source to the inlet orifice is adjustable. The configuration shown here is the most sensitive in calibrations with H_2SO_4 (see Section 3.1).

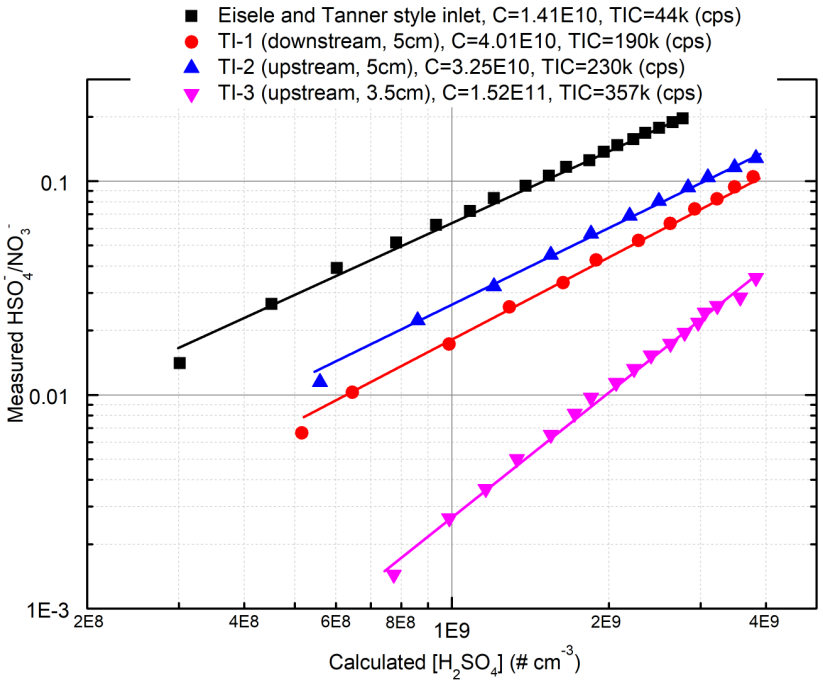

669

670 **Figure 3. Comparison of the sensitivities for the two inlets to H_2SO_4. The calibration process followed that reported by Kürten et al.**

671 **(2012) and is discussed in detail in the supplementary material. TI-1, 2, 3 represent different locations of the ion source relative to**

672 **the inlet orifice of the mass spectrometer. "upstream" and "downstream" indicated 0.5 cm upstream or downstream along the**

673 **sample flow axis and "3.5 cm" and "5 cm" indicate 3.5 or 5 cm away from the inlet orifice along the reagent ion flow axis.**

674

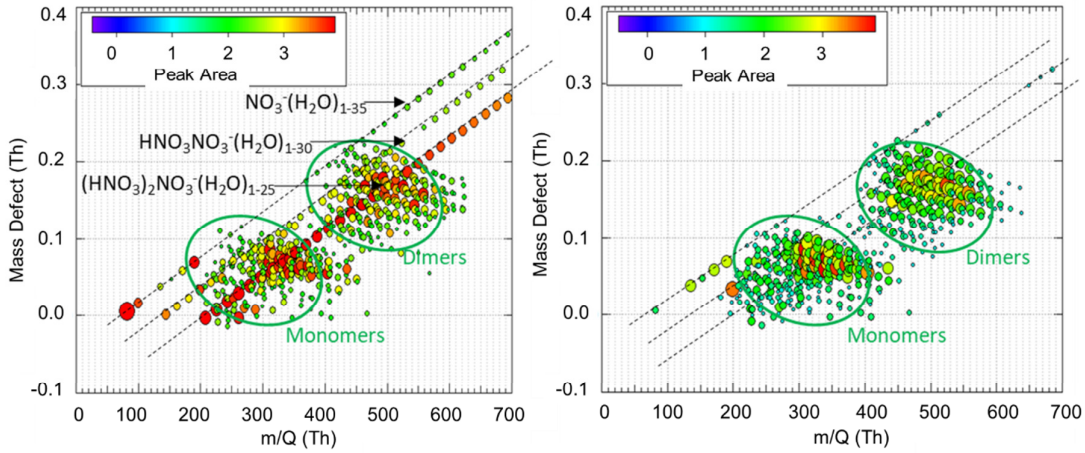

675

676 **Figure 4. Mass defect plots of α-pinene ozonolysis HOMs with 0 LPM (left) and 1 LPM (right) N_2 curtain gas flow when RH ≈ 85%,**

677 **with monomer and dimer HOMs circled in green. The most intense ions comprising 60% of the total ion count are plotted for**

678 **clarity. H_2O clusters $(H_2O)_m(HNO_3)_nNO_3^-$ (m = 1 - 35, n = 0 - 2) are circled in red in the left plot and are notably absent with the**

679 **application of the N_2 curtain gas. $(HNO_3)_2NO_3^-$ and $HNO_3NO_3^-$ are much more likely to cluster with H_2O than NO_3^-.**

680

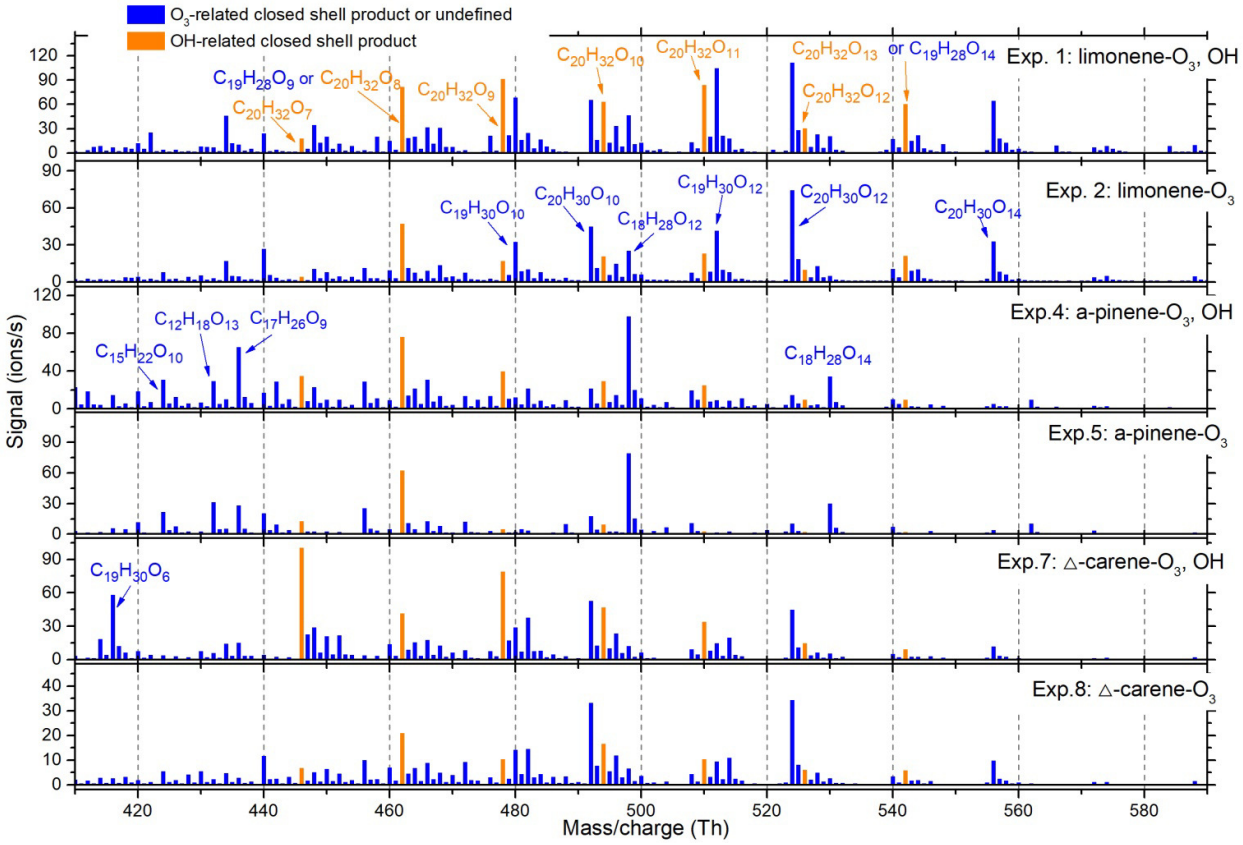

Figure 5. Average dimer mass spectrum in each of the particle generation experiments. The OH- and O_3-derived species were distinguished by comparing relative abundance of experiments with and without OH scavenger. All the peaks shown were in the form of adducts with NO_3^- or $HNO_3NO_3^-$ reagent ions.

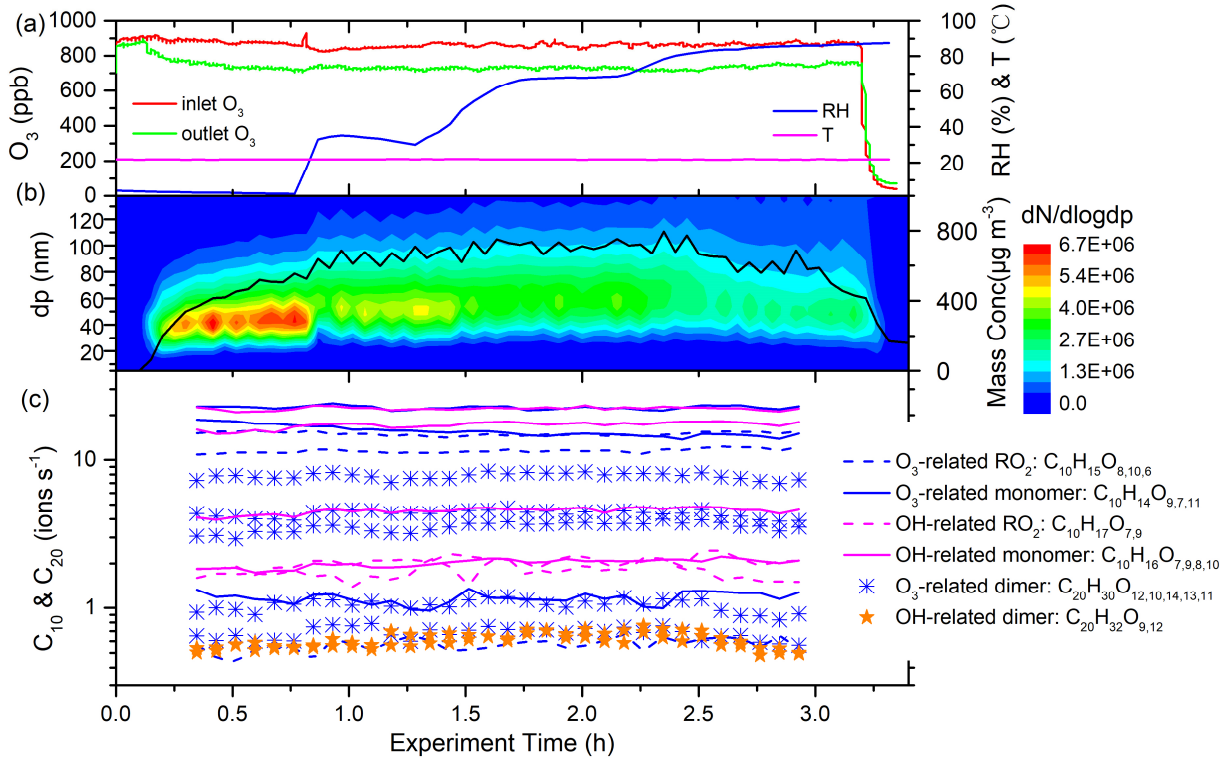

687

688 **Figure 6. Time series of experimental parameters, particle size distribution, and key ions during EXP. 2 (limonene oxidized by O_3**

689 **without OH scavenger). (a) inlet and outlet O_3 concentrations, temperature, and RH; (b) Particle size distribution and integrated**

690 **mass concentrations (assuming effective density is 1.2 g cm^{-3}); (c) Some of the main HOMs detected by TI-CIMS with NO_3^- reagent**

691 **ion. The subscript oxygen numbers in the formulae were ranked (left-to-right) according to signal abundance of the corresponding**

692 **molecule.**

693

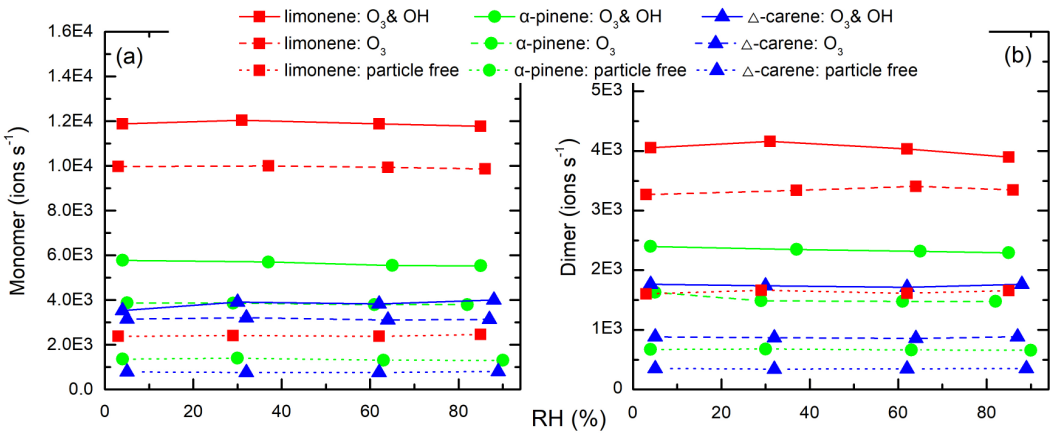

694

695 **Figure 7. Average (a) monomer and (b) dimer HOMs signal intensity (ions s^{-1}) as a function of RH in each experiment. Monomer**

696 **signals were the sum of $C_{5\text{-}10}$ molecules and dimer signals were the sum of $C_{15\text{-}20}$ molecules. No obvious signal change was seen for**

697 **increasing RH in any of the experiments.**

698

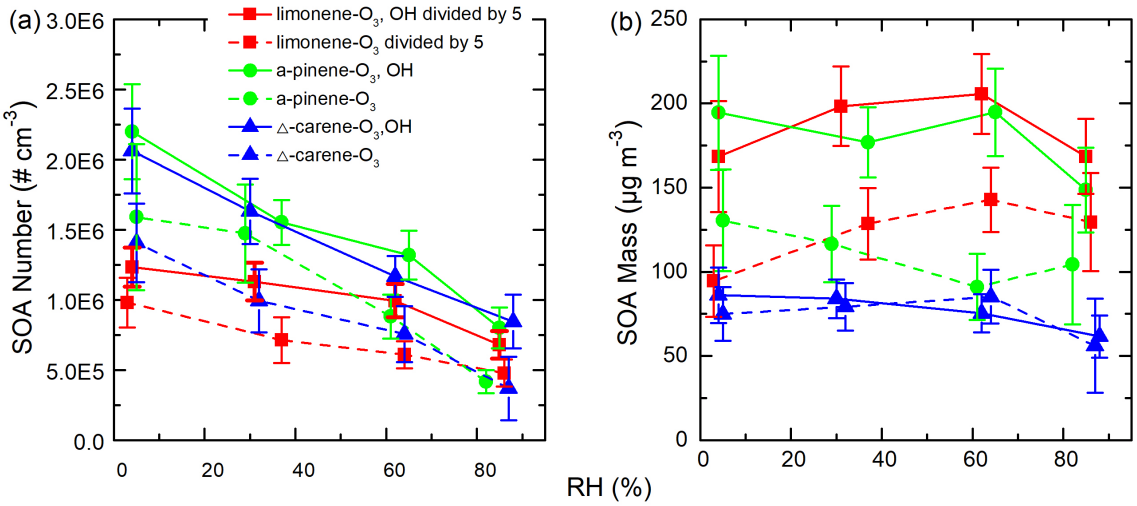

699

700 **Figure 8. SOA (a) number and (b) mass concentrations as a function of RH during different experiments. The error bars were**

701 **calculated using both the statistical errors of all individual size distributions during each RH stage and assuming a systematic CPC**

702 **counting error of 10%).**

703

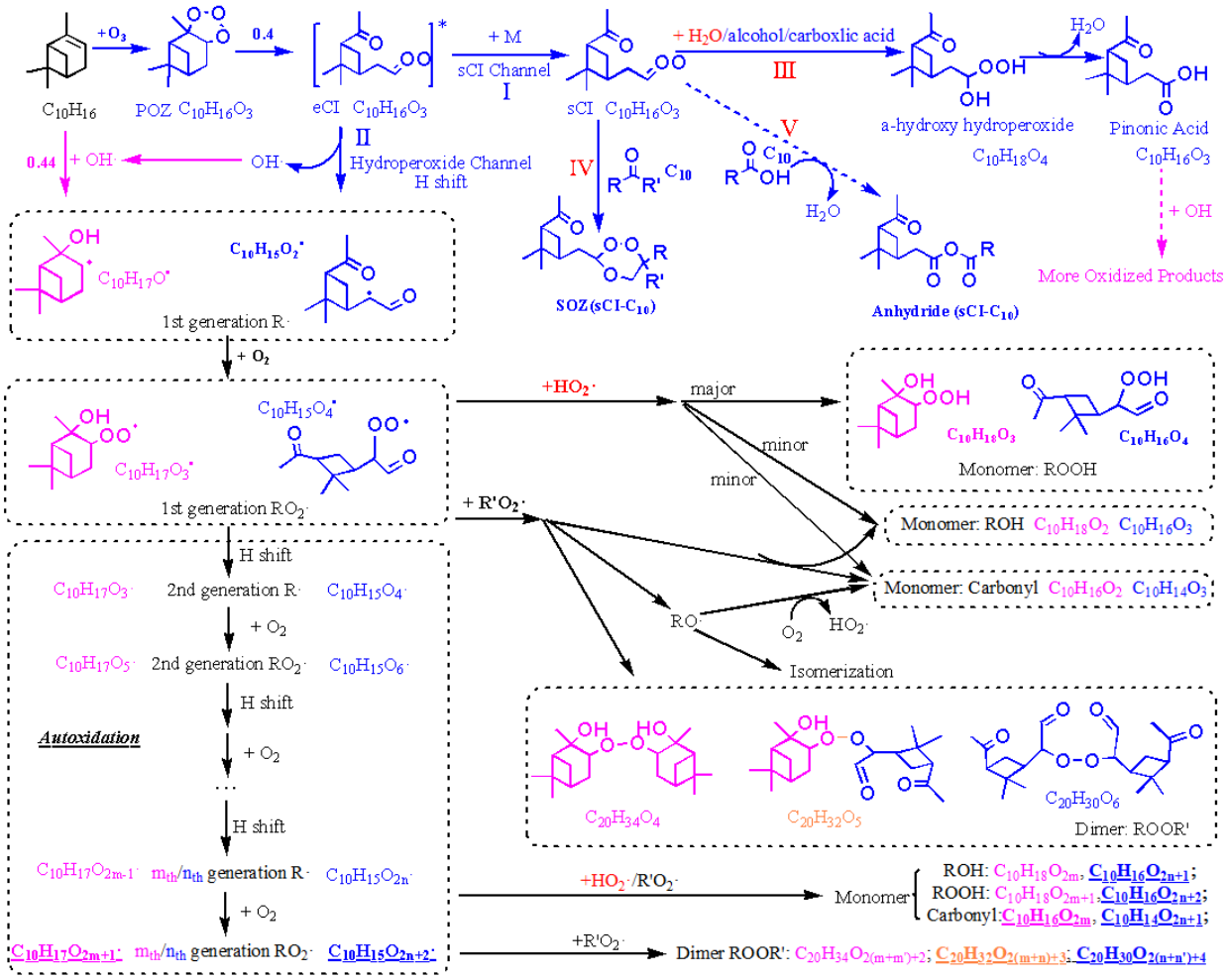

Figure 9. Proposed key steps in the formation of the representative C_{10} and C_{20} closed shell products from α-pinene oxidation and possible water vapor influence. Dashed lines represent pathways that may or may not happen, depending on the situation. Pink and blue colors represented the pathways or products from O_3 and OH oxidation, respectively. Common pathways or products are indicated in black type. Orange colors represented the combined products of O_3 and OH chemistry. Red colors highlight the direct or indirect influence of water. Underlined formulae were the main products observed from the mass spectrum. $C_{10}H_{18}O_{2m}$ and $C_{20}H_{34}O_{2(m+m')}$ were not observed in our spectrum, but they dominated the spectrum in other reported experiments where extra OH was generated (Berndt et al., 2016).

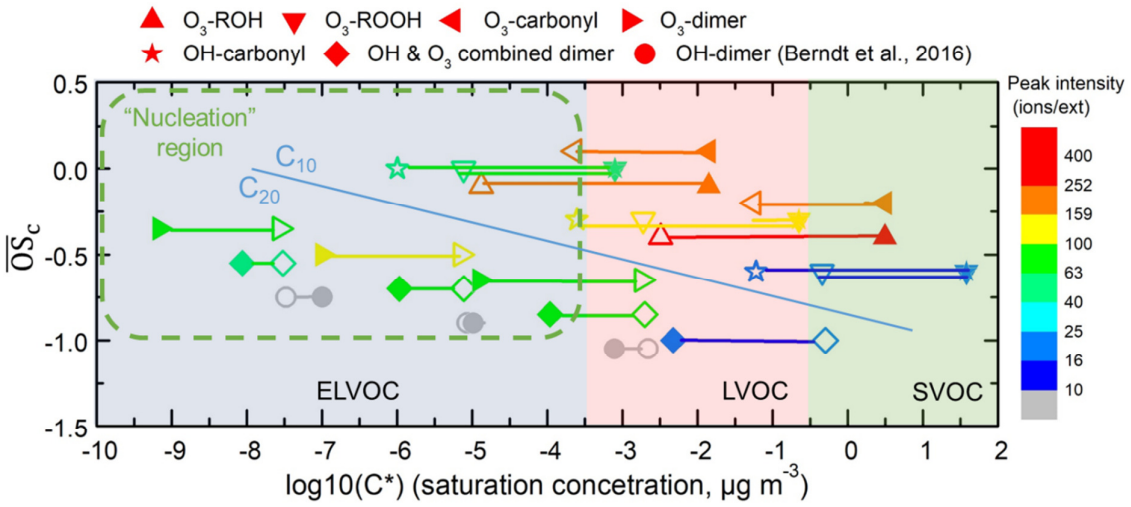

Figure 10. Vapor saturation mass concentration C* (T=298 K) of the major C_{10} and C_{20} closed shell products were predicted with SIMPOL.1 (open points) (Pankow and Asher, 2008) and Molecular Corridor method (filled points) (Li et al., 2016). Lines connecting the open points and filled points represent the difference between the two methods. O_3 or OH-derived, monomers and dimers are presented in different shapes. The peak intensity, represented by color, is from Exp.1 (limonene oxidation without OH scavenger). The gray points, which represent OH-derived dimers, are dominating products in OH initiated oxidation experiments (Berndt et al., 2016) while not observed in this study. Data used in this figure are given in Table S1. The nucleation region (green dashed rectangle) is from Donahue et al. (2013).

Supplemental Information: Relative Humidity Effect on the Formation of Highly Oxidized Molecules and New Particles during Monoterpene Oxidation

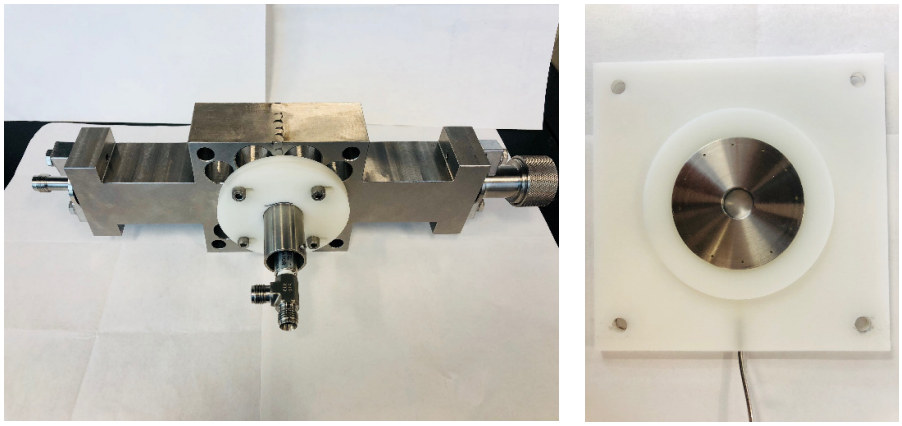

Figure S1. Photographs of the Transverse Ionization inlet (left) and the N_2 curtain gas plate (right).

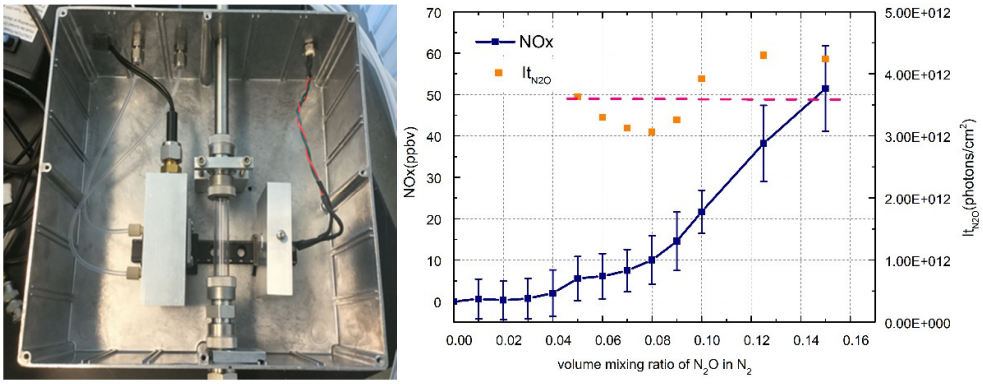

Figure S2. (Left) H_2SO_4 calibration system based on the design of Kurten et al. (Kurten et al., 2012). H_2SO_4 is generated by exposing known concentrations of gaseous SO_2, O_2, and H_2O to 185nm UV radiation produced by a mercury lamp (model 90-0012-01, Pen Ray) and a 185 nm bandpass filter (model XB32, 185BP20, Omega). Varying [H_2SO_4] was achieved under conditions of constant [SO_2] by varying [OH] in the system. OH is generated from the photolysis of water vapor. The water vapor concentration is calculated from the measured relative humidity (RH) and temperature. The [OH] in the system depends on both [H_2O] and the light strength, represented by *It* (amount of photons per cm^2), which is the product of the photon intensity *I* (amount of photons per second per cm^2) and the illumination time t_r (s).

(Right) Calibration of photodiode from the N_2O experiment. *It* was determined through chemical actinometry (N_2O to NOx conversion). The light strength was kept constant between photodiode calibration and H_2SO_4 calibration experiments, this was assured by measurements from a photodiode (model R5764, Hamamatsu) followed by an electrometer (model 485, Keithley). It_{N2O} was determined to be 3.85×10^{12} photons cm^{-2} when the photodiode current was 62nA. In the H_2SO_4 calibration experiment, all generated OH was transformed to H_2SO_4 within several milliseconds, 10% of [H_2SO_4] diffusion loss was applied to the 15 cm connection tube between the illumination area and the LTOF inlet. The generated [H_2SO_4] was constrained to above ~3×10^8 cm^{-3} because of the low detection limit of the RH sensor and the incomplete conversion of SO_3 to H_2SO_4 under low [OH]. (Kurten et al., 2012).

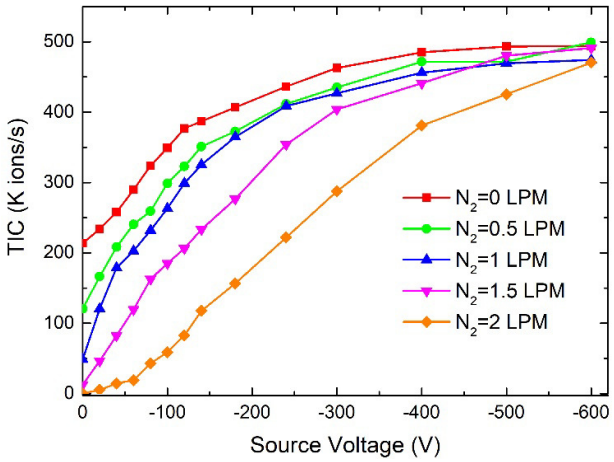

Figure S3. Total ion counts from the TI-CIMS as a function of ion source voltage at different curtain gas flow rates. As the ion source voltage increased, the voltage applied to the reaction chamber changed accordingly and always kept at half of the ion source voltage. A 1 LPM curtain gas flow rate and a -100V source voltage were used in our experiments.

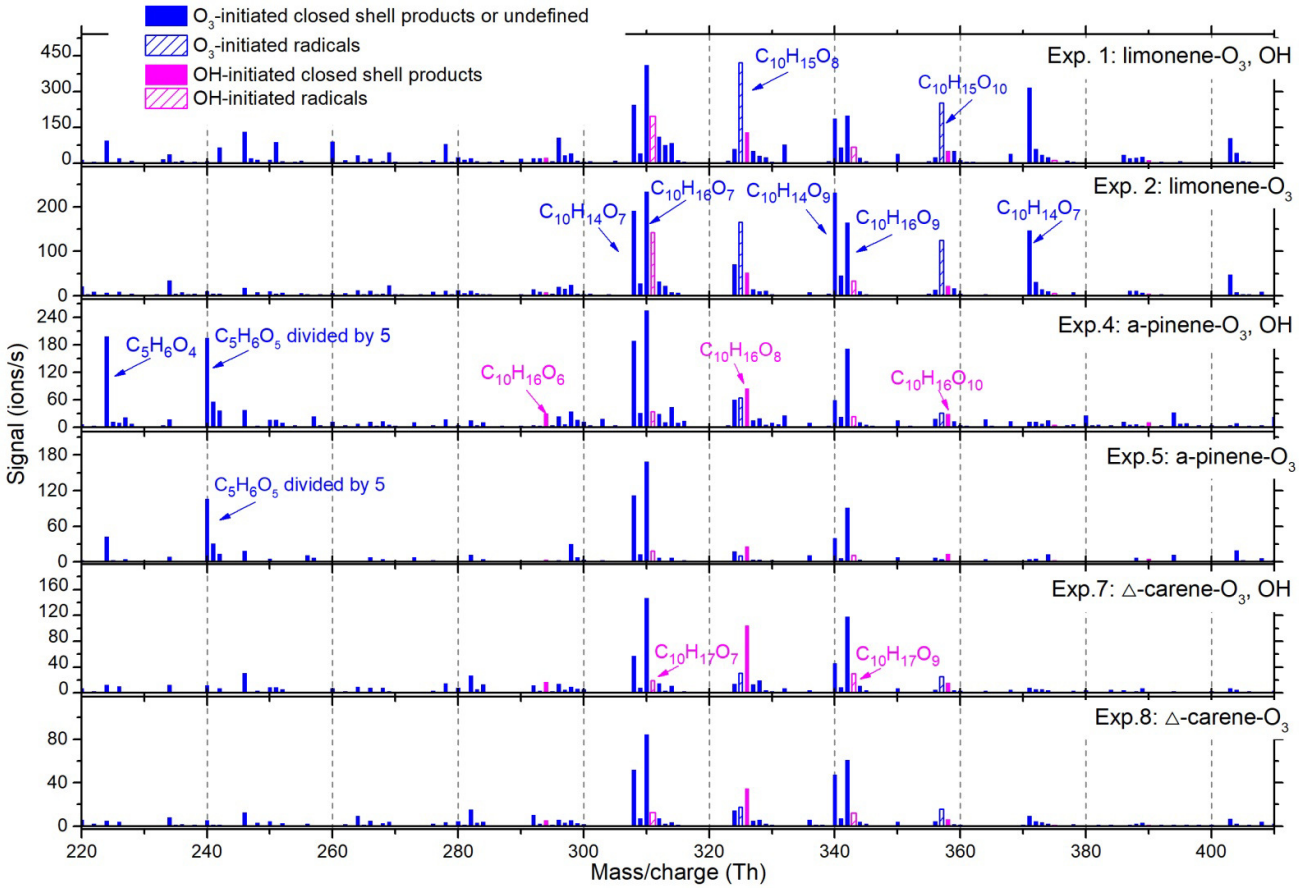

Figure S4. Averaged monomer and RO_2 radical mass spectra in six of the particle generation experiments. OH- and O_3-derived species were identified from previous studies (Jokinen et al., 2014). No significant differences were seen between experiments with and without OH scavengers. Peak labels are the identified neutral molecule, but the mass spectra show these compounds clustered with NO_3^- or $HNO_3NO_3^-$ reagent ions.

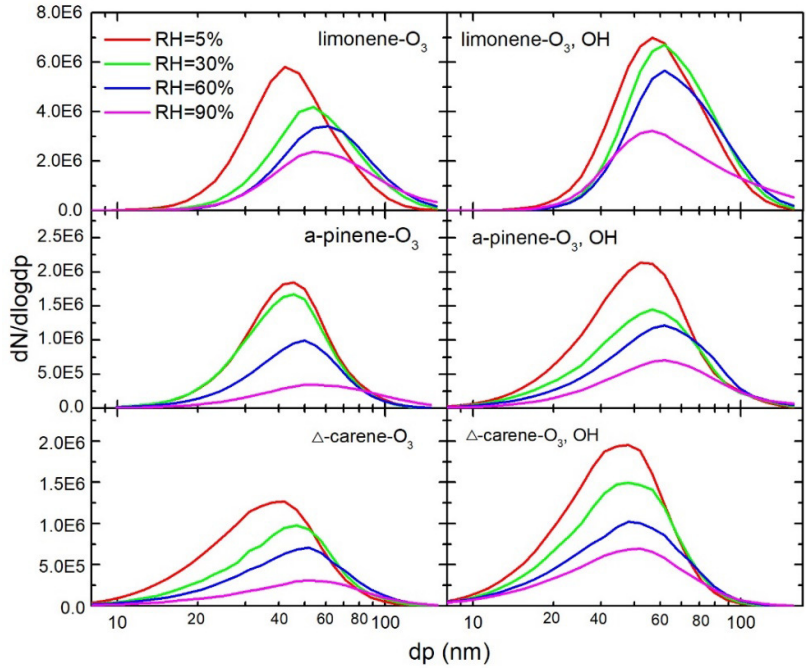

Figure S5. Averaged size distributions as a function of RH in each experiment.

Table S1. The Volatility of the major products were predicted with SIMPOL.1 (Pankow and Asher, 2008) and Molecular Corridor (298K) methods (Li et al., 2016).

	molecular	$\overline{OS_C}$	non-aromatic ring[1], b_4	-OH, b_7	-CH=O, b_8	-C=O-, b_9	-O-O-, b_{26}	-OOH, b_{27}	SIMPOL lgC*[2]	M-corridor lgC*	Peak area
O_3-ROH	$C_{10}H_{16}O_7$	-0.4	1	1	1	1	0	2	-2.49	0.5	412
	$C_{10}H_{16}O_9$	-0.1	1	1	1	1	0	3	-4.88	-1.85	199
O_3-ROOH	$C_{10}H_{16}O_6$	-0.6	1	0	1	1	0	2	-0.34	1.58	22
	$C_{10}H_{16}O_8$	-0.3	1	0	1	1	0	3	-2.72	-0.65	129
	$C_{10}H_{16}O_{10}$	0	1	0	1	1	0	4	-5.11	-3.10	51
O_3-carbony l	$C_{10}H_{14}O_7$	-0.2	1	0	1	2	0	2	-1.25	0.50	245
	$C_{10}H_{14}O_9$	0.1	1	0	1	2	0	3	-3.64	-1.85	187
O_3-dimer	$C_{20}H_{30}O_{10}$	-0.65	2	0	2	2	1	2	-2.74	-4.98	65
	$C_{20}H_{30}O_{12}$	-0.5	2	0	2	2	1	3	-5.15	-7.00	111
	$C_{20}H_{30}O_{14}$	-0.35	2	0	2	2	1	4	-7.56	-9.16	64
OH-carbon yl	$C_{10}H_{16}O_6$	-0.6	2	1	0	1	0	2	-1.22	1.58	22
	$C_{10}H_{16}O_8$	-0.3	2	1	0	1	0	3	-3.60	-0.65	129
	$C_{10}H_{16}O_{10}$	0	2	1	0	1	0	4	-5.99	-3.1	51
OH&O_3-di mer	$C_{20}H_{32}O_7$	-1	3	1	1	1	1	1	-0.29	-2.32	18
	$C_{20}H_{32}O_9$	-0.85	3	1	1	1	1	2	-2.70	-4.04	91
	$C_{20}H_{32}O_{11}$	-0.7	3	1	1	1	1	3	-5.11	-5.97	84
	$C_{20}H_{32}O_{13}$	-0.55	3	1	1	1	1	4	-7.52	-8.06	60
OH-dimer	$C_{20}H_{34}O_8$	-1.05	4	2	0	0	1	2	-2.66	-3.15	--
	$C_{20}H_{34}O_{10}$	-0.9	4	2	0	0	1	3	-5.07	-4.98	--
	$C_{20}H_{34}O_{12}$	-0.75	4	2	0	0	1	4	-7.47	-7.00	--

[1]The functional groups used here were directly predicted from the proposed formation pathways in Figure 9 and did not include the intramolecular isomerization, like ring closure of unsaturated RO_2 (Berndt et al., 2016).

[2]At T=298K, the parameters in SIMPOL.1 were b_0 = 1.842, b_4 = -0.021, b_7 = -2.183, b_8 = -1.320, b_9 = -0.937, b_{26} = -0.392, and b_{27} = -2.440. The equation used for volatility calculation is $log_{10}P^0_{L,i}(T) = \sum_k v_{k,i} b_k(T)$, where $P^0_{L,i}(T)$ is the liquid vapor pressure of the compound. $v_{k,i}$ is the number of groups of type k, and $b_k(T)$ is the contribution by each group of type k. (Pankow and Asher, 2008).

References cited

Berndt, T., Richters, S., Jokinen, T., Hyttinen, N., Kurtén, T., Otkjær, R. V., Kjaergaard, H. G., Stratmann, F., Herrmann, H., and Sipilä, M.: Hydroxyl radical-induced formation of highly oxidized organic compounds, Nature communications, 7, 13677, 2016.

Jokinen, T., Sipilä, M., Richters, S., Kerminen, V. M., Paasonen, P., Stratmann, F., Worsnop, D., Kulmala, M., Ehn, M., and Herrmann, H.: Rapid autoxidation forms highly oxidized RO2 radicals in the atmosphere, Angewandte Chemie International Edition, 53, 14596-14600, 2014.

Kurten, A., Rondo, L., Ehrhart, S., and Curtius, J.: Calibration of a Chemical Ionization Mass Spectrometer for the Measurement of Gaseous Sulfuric Acid, J Phys Chem A, 116, 6375-6386, 2012.

Li, Y., Pöschl, U., and Shiraiwa, M.: Molecular corridors and parameterizations of volatility in the chemical evolution of organic aerosols, Atmos Chem Phys, 16, 3327-3344, 2016.

Pankow, J. F., and Asher, W. E.: SIMPOL. 1: a simple group contribution method for predicting vapor pressures and enthalpies of vaporization of multifunctional organic compounds, Atmos Chem Phys, 8, 2773-2796, 2008.